

07

Advanced Optical Metrology

Geoscience



OLYMPUS

WILEY

Contents

- 3** Geoscience
- 7** Portable X-Ray Fluorescence Spectrometry Analysis of Soils
D. C. Weindorf and S. Chakraborty
- 13** Impact of Sample Preparation Methods for Characterizing the Geochemistry of Soils and Sediments by Portable X-Ray Fluorescence
K. Goff, R. J. Schaetzel, S. Chakraborty, et al.
- 20** Semiquantitative Evaluation of Secondary Carbonates via Portable X-Ray Fluorescence Spectrometry
S. Chakraborty, D. C. Weindorf, C. A. Weindorf, et al.
- 26** Using EMI and P-XRF to Characterize the Magnetic Properties and the Concentration of Metals in Soils Formed over Different Lithologies
S. Doolittle, J. Chibirka, E. Muñiz, et al.
- 33** XRF and XRD Instruments for Geoscience

Imprint

© Wiley-VCH GmbH
Boschstr. 12,
69469 Weinheim, Germany
Email: info@wiley-vch.de
Editor-in-Chief: Dr. Christina Poggel

Geoscience

Geoscience is the scientific study of the Earth — more precisely, the study of the materials, structures, evolution, and dynamics of the Earth, including its organisms, natural minerals, and energy resources. Geoscientists routinely investigate the composition and molecular structure of soils, rocks, sediments, minerals, and other geological samples. Geoscientists employ many analytical techniques to characterize these materials and samples — among them X-ray analytical techniques such as X-ray fluorescence (XRF) and X-ray diffractometry (XRD) [1,2].

XRF is the most frequently used analysis technique for determining the elemental composition of rock, sediment, and other earth material samples [3]. In XRF, the sample is bombarded with a high-energy X-ray beam, leading to the ionization of its component atoms and the dislodgment of an inner-shell electron. The resulting electron-hole in the inner shell is then filled by an outer-shell electron accompanied by the release of energy in the form of a photon. The emitted radiation has a lower energy than the absorbed radiation and is termed 'fluorescence'. The energy of the emitted radiation reflects the energy difference between the two shells involved. As these transitions occur at discrete energies unique to a specific element and its local environment, the emitted characteristic fluorescence can be used to determine the elements in a sample and after calibration, its concentration. Thus, XRF analysis can determine the elemental/chemical composition of a sample but fails to differentiate between the different compounds present in the sample.

Like XRF, XRD measures the response of X-rays interacting with a sample to identify substances. XRD leverages the fact that crystalline materials (e.g., minerals) exhibit a certain degree of periodicity in their structural arrangement [4]. When a monochromatic X-ray beam

irradiates a crystalline sample, the X-rays collide with the sample's electrons, leading to constructive interference (i.e., diffraction) as long as the Bragg's Law ($n\lambda = 2d \sin\theta$) is satisfied. The law relates the wavelength of the incident beam to the diffraction angle and the distance between the lattice planes of the atoms arranged in the crystalline sample. Each material produces a unique diffraction pattern by which it can be identified. Such diffraction patterns can be compared and matched with those of known structures (e.g., various minerals) maintained in the International Center for Diffraction Data (ICDD) database. In contrast to XRF, XRD identifies and quantifies crystalline compounds or phases in a sample and determines its degree of crystallinity and amorphous content. Thus, the methods are complementary to each other. For example, XRF could measure the total concentration of a specific element (e.g., Ca) in a given geological sample, while XRD could determine and differentiate between the compounds in which this element exists (e.g., CaO vs. CaCO₃).

Both techniques have been widely applied in different fields of geoscience for decades, with portable versions of XRF and XRD (pXRF and pXRD, respectively) allowing for fast in situ screenings and analyses [5].

This introduction will briefly describe the advances in pXRF and pXRD, the implication of both methods for geoscience, and their application in soil and rock analysis. The following digest articles will focus on the application of pXRF in geological settings.

1. ADVANCES IN PXRF AND PXRD AND THEIR IMPLICATIONS FOR GEOSCIENCE

With advancements in hardware and software technologies (i.e., X-ray tubes, detectors, and processors), pXRF and pXRD devices have become important qualitative and quantitative characterization tools for analyzing geological materials.

Early pXRF spectrometers usually comprised radioactive isotopes as their excitation source and Si-PIN diode detectors, but in later gen-

erations, the radioactive isotope sources and PIN diode detectors were replaced by small X-ray tubes and silicon drift detectors, respectively^[3,7]. Several generations of improvement have led to the current standard for pXRF, featuring relatively low detection limits, high sensitivity, low background noise, high temperature stability, high resolution at high count rates, and fast processing times. Portable XRF devices have many advantages over traditional lab-based techniques, including, of course, portability, allowing for *in situ* data collection; little to no sample preparation, facilitating the scanning process; wide dynamic range and multi-element capability, enabling accurate and precise quantification of many elements; and speed, allowing for fast decision-making on site. Moreover, pXRF is a non-destructive technique, allowing for multiple measurements of the same sample and the use of analyzed samples for future use. Using a pXRF device, geoscientists can quickly cover large study areas, increasing the sampling density and advancing decision-making. Modern pXRF devices have integrated GPS receivers that are used to georeference the collected data, enabling rapid spatial visualization using a geographic information system (<https://www.olympus-ims.com/en/handheld-xrf-for-soil-surveys-geochemistry-of-rock-outcrops-soils-and-sediments/>).

Due to these beneficial properties, pXRF devices are widely used in geoscience. Besides the scientific and experimental benefits, pXRF is a highly cost-effective technique; according to an ASX-listed explorer, a saving of \$2.75 million over a three-year period was achieved by employing pXRF devices for testing 100,000 samples instead of costly lab-based techniques (<https://www.olympus-ims.com/en/handheld-xrf-for-soil-surveys-geochemistry-of-rock-outcrops-soils-and-sediments/>). Likewise, the First Mining Finance Corporation used pXRF devices for assessing soil geochemistry within their Sonora projects (Mexico); the estimated costs were approximately 3–5 times less than those of traditional wet chemistry analysis at commercial labs (<https://www.olympus-ims.com/en/customer-case-study-soil-geochemistry-by-pxrf-at-the-sonora-project-mexico/>).

The digest article “Portable X-ray fluorescence spectrometry analysis of soils” reviews further advantages and disadvantages of pXRF and provides helpful, practical tips and recommendations for its application in the geoscientific field. The remaining digest articles in this eBook demonstrate the high quality of pXRF data obtained from geo-

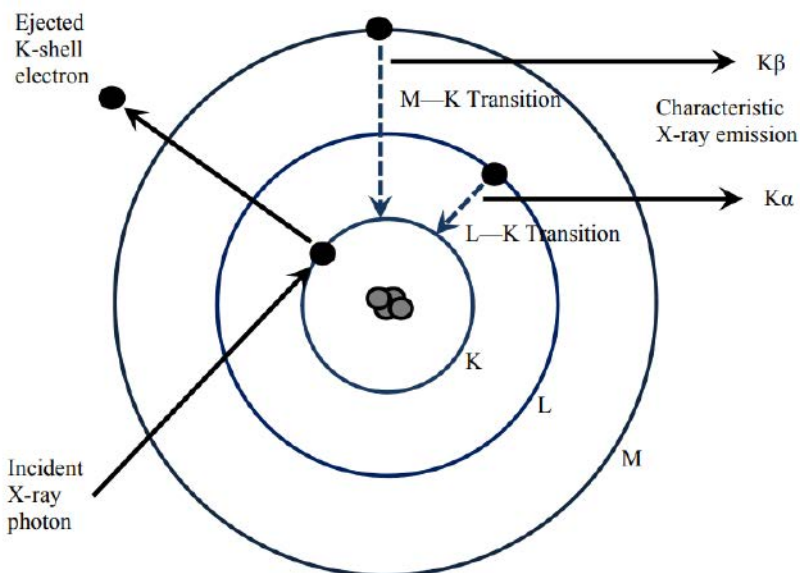


Figure 1: Fundamental principles of XRF. When an electron void in the K shell is filled by an electron from the L or M shell, the emitted photon is termed $K\alpha$ or $K\beta$, respectively. The figure is taken from reference^[6].

scientific samples, which are comparable to those of traditional analytical techniques.

Like pXRF, pXRD has benefited from technological advances, especially from the automation of data processing and the use of vibrating sample holders and CCD-based cameras. Portable XRD devices now offer fast, accurate, and cost-effective analysis of geological samples [5]. Although pXRD devices are larger and heavier than handheld pXRF devices, they can be operated in the field. The ability to identify minerals in situ by pXRD promotes more accurate geological logging and provides valuable insights into geological systems. In contrast to pXRF, pXRD is generally limited to crystalline materials and is thus primarily used for the characterization and identification of crystalline materials in soils and sediments. Nonetheless, it is a commonly used and proven technique to identify and quantify the mineralogical composition of raw materials [8]. However, geoscientists have concluded that pXRD data alone is insufficient for soil mineral identification and thus should be combined with other techniques [9].

2. APPLICATION OF PXRF AND PXRD IN SOIL AND ROCK ANALYSIS

Given the importance of the elemental composition of soils and rocks, the application of pXRF is rapidly expanding in soil and rock analysis. The obtained elemental data can be used to predict soil and rock physical and chemical properties, such as salinity, pH, and cation-exchange capability [3]. Gazley *et al.* [10] presented a rapid and robust pXRF-based workflow to aid exploration in a regolith-dominated terrane. The authors obtained a large dataset from the Western Mount Isa Inlier, Queensland, Australia, including data from soil, rock, and rotary air blast samples. Portable XRF data obtained from the soil samples were comparable to laboratory data for most elements (Cu and Zn within 2% of laboratory data; Mn, Rb, and Sr within 8% of laboratory data; and Fe, Al, K, and Ca within 25% of laboratory data). However, the Pb content in the soil estimated by pXRF was 77% less than that estimated by the laboratory. This underestimation was due to an erroneous Pb concentration reported by the pXRF device because of energy peaks overlap between Fe (pile up) and Pb. The rotary air blast dataset showed a similar trend to the soil dataset (Pb overestimated by 69%), and the rock dataset, which was uncorrected, correlated unexpectedly well

with the laboratory data for many elements. Thus, the authors concluded that the use of pXRF enables dynamic exploration campaigns in regolith-dominated terranes at a relatively low cost, with decision-making being possible while the drill rig is still in the study area.

Ahmed *et al.* [11] used pXRF to evaluate the ore-forming potential of intrusive rocks in different porphyry Cu environments by assessing their Sr/Y and Sr/MnO contents, which are effective discriminators between ore-forming and unprospective intrusions. For this purpose, pXRF data were collected from pulp powders and rock slabs from six porphyry Cu districts. Calibrated pXRF data obtained from pulp powders correlated very well with those of conventional methods (within 16%). In contrast, pXRF data obtained from rock slabs correlated less well with those of conventional methods (within 37%). This discrepancy in the data between the samples was due to homogeneity differences (in terms of grain size and mineralogy) between pulp powder and rock slabs. Nevertheless, pXRF represents a rapid and cost-effective alternative to traditional methods for collecting Sr, Mn, and Y data to determine the ore-forming potential of intrusions.

Portable XRF can also be applied in geological oceanography to study the geological history of the ocean floor. Ivanova *et al.* [12] used pXRF, in combination with other techniques, to analyze the sediment cores from the summit and the northeastern slope of the Ioffe Drift, which is located in the Antarctic Bottom Water pathway. The study was conducted to identify hiatuses in the contourite records, determine their duration, and refine the stratigraphy of the upper sediment cover overlaying the Ioffe Drift area. The Ca/Ti and Ca/Al ratios were determined by pXRF as they represent biogenic/terrigenous material ratios, reflecting the changes in terrigenous sediment contribution. Abrupt changes in the XRF data were used to infer potential long- and short-term hiatus/erosional events over the last ~ 3 million years. The authors demonstrated that continuous pXRF scanning, in combination with other techniques, is an excellent approach to identifying hiatuses, even short-lived ones.

Portable XRD is particularly useful for on-site mineralogical analysis and geological exploration. For example, in the Indika project, pXRD was used for testing critical mineral identification in two study areas in northern Finland [13]. Using pXRD, the authors successfully detected common rock-forming minerals, such

as albite, amphiboles, muscovite, and quartz, and indicator minerals for both study areas in till and weathered bedrock samples. However, as mentioned before, the authors also noted that the pXRD data alone was not reliable enough without employing complementary methods. Another study demonstrated that pXRD could be applied to identify hydrothermally modified mineral fissures, which can be used to track the formation conditions for ore deposits and other geothermal systems^[14].

Besides being largely used individually, pXRF and pXRD were also combined to investigate a large set of complex geological samples^[15]. Coupled pXRF-pXRD analysis delivered both elemental (XRF) and mineralogical (XRD) information of high quality, making it a promising method for the exploration of lithologies, hydrothermal alterations, and ores.

REFERENCES:

- [1] T. D. T. Oyedotun, *Geol Ecol. Landsc.* 2018, 2, 148.
- [2] B. Lavina, P. Dera, R. T. Downs, *Rev. Mineral. Geochem.* 2014, 78, 1.
- [3] D. C. Weindorf, N. Bakr, Y. Zhu, *Adv. Agron.* 2014, 128, 1.
- [4] D. M. Moore, R. C. Reynolds Jr., in *X-Ray diffraction and the identification and analysis of clay minerals*, Oxford University Press, New York, 1997.
- [5] B. Lamiere, Y. A. Uvarova, *Geochem. Explor. Env. A.* 2020, 20, 205.
- [6] D. J. Kalnicky, R. Singhvi, *J. Hazard. Mat.* 2001, 83, 93.
- [7] D. C. Weindorf, S. Chakraborty, *Soil Sci. Soc. Am. J.* 2020, 84, 1384.
- [8] P. S. Nayak, B. K. Singh, *Bull. Mater. Sci.* 2007, 30, 235.
- [9] V. Singh, H. M. Agrawal, *Radiat. Phys. Chem.* 2012, 81, 1796.
- [10] M. F. Gazley, L. C. Bonnett, L. A. Fisher, W. Salama, J. H. Price, *Aus. J. Earth Sci.* 2017, 64, 903.
- [11] A. Ahmed, A. J. Crawford, C. Leslie, J. Phillips, T. Wells, A. Garay, S. B. Hood, D. R. Cooke, *Geochem. Explor. Env. A.* 2020, 20, 81.
- [12] E. Ivanova, D. Borisov, O. Dmitrenko, I. Murdmaa, *Mar. Pet. Geol.* 2020, 111, 624.
- [13] P. Sarala, H. Koskinen, *Geologi* 2018, 70, 58.
- [14] D. A. Burkett, I. T. Graham, C. R. Ward, *Canad. Mineral.* 2015, 53, 429.
- [15] Y. A. Uvarova, J. S. Cleverly, A. Baensch, M. Verrall, *Coupled XRF and XRD analyses for efficient and rapid characterization of geological materials: Applications for the mineral exploration and mining industry, conference paper at the 21st General Meeting of the International Mineralogical Association (IMA), Johannesburg, 2014.*

01 Portable X-Ray Fluorescence Spectrometry Analysis of Soils

D. C. Weindorf and S. Chakraborty

ABSTRACT

Portable X-ray fluorescence (pXRF) spectrometry is a proximal sensing technique whereby low-power X-rays are used to make elemental determinations in soils. The technique is rapid, portable, and provides multi-elemental analysis with results generally comparable to traditional laboratory-based techniques. Elemental data from pXRF can then be either used directly for soil parameter assessment or as a proxy for predicting other soil parameters of interest via simple or multiple linear regression. Importantly, pXRF has some limitations that must be considered in the context of soil analysis. Notwithstanding those limitations, pXRF has proven effective in numerous agronomic, pedological, and environmental quality assessment applications.

RATIONALE FOR GENERAL PROCEDURE

The elemental composition of soil is one of its most fundamental chemical parameters, affecting its reaction, salinity, cation-exchange capacity (CEC), nutrient cycling, and pollutant transport. Early forays into soil chemical analysis relied on colorimetric wet chemistry methods such as titration or colorimetry^[1]. In recent decades, these simplistic measurements gave way to methods offering greater accuracy and precision: atomic absorption spectrometry (AAS) and inductively coupled plasma atomic emission spectroscopy (ICP–AES). While the latter is the analytical standard for contemporary elemental analysis, both methods have some limitations; specifically, they require digestion of soil with caustic chemicals such as nitric or hydrochloric acids for partial digestion^[2] or hydrofluoric acid for

total digestion^[3]. Therefore, these approaches require considerable time, energy, consumables, and laboratory-based equipment.

By contrast, X-ray fluorescence (XRF) was originally developed as a laboratory-based technique^[4], but it has since been miniaturized into small, portable units capable of making quality elemental determinations in situ with minimal sample preprocessing. The energies of most X-rays reflect the core-electron-binding energies of atoms; thus, the atomic number strongly influences XRF effectiveness^[5]. XRF describes the emission of fluorescent photons from a sample that has been irradiated by high-energy X-rays. As the emitted (fluorescent) secondary X-rays have discrete energies unique to a particular element and its local environment, X-ray absorption (or emission) can be used for elemental determination in soils. Using the rela-

tionship between emission wavelength and atomic number, specific elements can be identified and quantified in a sample [6].

Early portable XRF (pXRF) instruments often featured radioactive isotopes as their excitation sources (e.g., Cd¹⁰⁹ or Fe⁵⁵) and featured Si-PIN diode detectors [6]. In later generations, these radioactive isotope sources were replaced by miniaturized tube-based X-ray sources, and Si-PIN diodes were replaced by silicon drift detectors, with the latter presenting tremendous advances in pXRF accuracy and precision. For purposes of discussion and methodology, all comments hereafter refer to experiences with an Olympus® DELTA™ Premium (DP-6000) pXRF configured with a 4 W Rh X-ray tube operated at 10–40 keV.

based methods but also some limitations. One of the greatest advantages of pXRF is its field portability as it is configured as a handheld meter that can be taken to the field for in situ soil analysis. Scanning time varies widely but is typically in the order of ~60 to 90 seconds. Longer scanning times (up to 300 seconds) increase the accuracy of elemental readings. Also, pXRF can be operated by rechargeable Li-ion batteries, thus requiring no conventional electrical power supply on-site. Portable XRF offers a wide dynamic range of elemental quantification from low mg kg⁻¹ to high percentage levels, with no need for dilutions or restandardization. Lastly, pXRF analysis is multi-elemental, providing simultaneous analysis of ~20 elements. However, the detection limits of each element vary based on the atomic number and size of the electron cloud. Generally, elements with larger atomic numbers are measured more accurately than those with lower ones. For example, light elements such as P might have a limit of detection (LOD) of ~±5000 mg kg⁻¹, whereas heavy elements such as U might have a LOD of ± 5 mg kg⁻¹ (Figure 1).

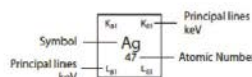
Figure 1: Periodic table of elements showing LODs for Olympus X-ray fluorescence analyzers.

REVIEW OF EXISTING PROCEDURES: STRENGTHS, LIMITATIONS, INTERFERENCES

The use of pXRF for soil analysis offers many strengths relative to traditional laboratory-



Alloy Analysis:
 Elements detected: Magnesium (Mg, Z=12) through Sulfur (S, Z=16) and Titanium (Ti, Z=22) through Plutonium (Pu, Z=94).



Detection limits are a function of testing time, sample matrix and presence of interfering element. Detection limits are estimates based on 1-2 minutes test times and detection confidence of 3σ (99.7% confidence). Interference-free detection limits are intended as guidelines: please contact Olympus Innov-X to discuss your specific application.

Please see separate Alloy Analysis LOD Specifications.



INDIVIDUAL STEPS IN THE PREFERRED ANALYSIS, INCLUDING JUSTIFICATION

When conducting pXRF analysis of soil samples, several variables must be considered for optimal performance. First, the instrument must be properly standardized. The Olympus® DELTA™ pXRF features a calibration alloy clip (316 clip). Scanning the clip allows the instrument to lock into a standardized substance recognized by the integrated computer. Given the inherent heterogeneity in many soil samples, steps must be taken to ensure that pXRF scanning adequately reflects the composition of the soil being evaluated. When scanning in situ, the soil should be evaluated for concretions, nodules, or irregularities that may disproportionately affect pXRF performance; such areas should be avoided. The nose of the pXRF should be placed in direct contact with the soil, such that it makes good contact with a flat surface. In some instances, this may involve using a knife to gently scrape the soil to create a flat surface for scanning. To adequately capture variability within a given soil horizon, investigators should take multiple scans, physically repositioning the instrument between each scan to collect data on multiple points within a horizon. Excessive soil moisture ($\geq 20\%$) denudes fluorescence received by the instrument^[9]; thus, field evaluation of soil is best undertaken when soils are dry. In addition to scanning soil profiles, it can be convenient to scan soil cores collected with a hydraulic probe; the evaluation slot of the collection tube nicely accommodates the instrument's aperture (**Figure 2**). If field measurements are not essential, it may be preferable to scan soil samples ex situ after drying and grinding. Ex situ processing achieves two goals: reduction/elimination of soil moisture and sample homogenization. Scanning time is an important consideration as a longer scanning time produces optimized results. However, investigators must evaluate the need for reasonable sample throughput versus pXRF accuracy. Many soil evaluations typically use between 60 and 90 seconds for scanning^[4]. A good practice for evaluating the quality of pXRF data is to scan the National Institute of Standards and Technology (NIST)-certified reference soil standards. A recovery percentage (pXRF determined/NIST-certified value) can then be calculated and reported with the pXRF data collected. Notably, pXRF tends to over- or underreport some elements, but many elements achieve results within 10% of NIST-certified values.

Figure 2: Hydraulic probe sampling tube with slot accommodating the aperture of a pXRF device for field scanning at fixed depths.

Despite numerous advantages, pXRF has several limitations. First, pXRF is variably affected by soil moisture. Literature points to a critical value of 20% moisture, a threshold above which drying or moisture correction should be considered. Weindorf et al.^[7] noted that pXRF data quality was substantively reduced when evaluating frozen soils laden with ice relative to their dry counterparts.

Second, interelemental interferences are well documented. For example, As and Pb feature a shared spectral peak, making isolation and identification cumbersome^[8]. Importantly, pXRF fails to distinguish elemental valence (e.g., Fe^{2+} vs. Fe^{3+}) and merely reports total elemental concentration. Portable XRF also cannot read light elements (e.g., $Z \leq 11$ Na). This is particularly limiting in soil analysis when the consideration of Na is important. However, some contemporary approaches have sought to overcome those limitations using other elemental data as proxies for the light elements of interest. In most pXRF instruments, the aperture through which X-rays are emitted and fluorescence is detected is relatively small (~ 2 cm). Applied to highly heterogeneous matrices in soils, results can vary dramatically over only a few lateral centimeters in a soil profile. Finally, pXRF lacks very low LODs (very low or high mg kg^{-1}) required for some investigations, where AAS or ICP-AES will remain the analytical standard for the foreseeable future.



Figure 3: Hands-free pXRF operation using a hooded sample stage for special applications (left) and a bipod stand (right).

Although most instruments operate at low power (10–40 KeV), the operator must undergo proper radiation safety training to ensure safe operation as pXRF still produces ionizing radiation. The penetration depth of the X-rays produced by pXRF instruments is commonly a few mm. Thus, exposing skin or body parts to X-rays should be avoided. Furthermore, many states have licensing requirements for the use of radiation-producing devices that sometimes require the operator to wear a dosimetry badge to monitor X-ray exposure levels. Leakage of X-rays, which can be detected with a Geiger counter, most commonly occurs near the instrument's aperture if it fails to make planar contact with the sample being scanned. For comfort in prolonged use or specialized scanning applications, a bipod or sample stage can be used to position the pXRF for hands-free operation (**Figure 3**).

DATA QUALITY AND PROCESSING

Portable XRF for in-field environmental studies has repeatedly proven useful for directly predicting metal concentrations in soil. For example, Radu and Diamond^[10] reported strong coefficients of determination (R^2) for Pb (0.99), As (0.99), Cu (0.95), and Zn (0.84) between pXRF and AAS. Furthermore, pXRF has shown potential for environmental quality assessment of peri-urban agriculture, exhibiting reasonably strong correlations with ICP results of several trace elements^[11]. How-

ever, pXRF elemental data can also be used as a proxy for predicting other soil properties.

Traditionally, scientists have utilized simple linear regression (SLR) and multiple linear regression (MLR) for establishing correlations between pXRF measured elements and physicochemical soil properties measured via standard laboratory procedures. For example, Sharma et al.^[12] used pXRF for pH determination using elemental data as a proxy for soil pH. They used SLR and MLR to develop models associating pure elemental data from pXRF and pXRF elemental data with auxiliary input data (clay content, sand content, organic matter content). While MLR with auxiliary input data produced the best predictive model ($R^2 = 0.82$; RMSE = 0.541), MLR with pure pXRF elemental data provided a reasonable predictability ($R^2 = 0.77$; RMSE = 0.685). Notably, SLR could not produce a robust predictive model. Several other studies also included the development of SLR and/or MLR models (with or without auxiliary input data) to predict and find correlations between pXRF elemental data and traditionally lab-measured soil properties, such as soil CEC^[13], soil salinity (electrical conductivity)^[14], and soil gypsum content^[15]. In all cases, the model(s) produced at least acceptable R^2 values, ranging from 0.83 to 0.95 (see the full article for a complete reference list and detailed description of the studies).

Both SLR and MLR are commonly used techniques relating pXRF elemental data to standard laboratory characterization data for the physicochemical parameters of

interest. We recommend splitting the datasets into modeling (~70%) and validation (~30%) datasets when constructing a predictive model to assess model performance before using on unknown samples.

RECOMMENDATIONS

For common soil studies, *ex situ* scanning in the laboratory after drying and grinding of soil samples is preferable as this eliminates potential interference from soil moisture and provides increased sample homogeneity. As a balance between analytical accuracy and sufficient sample processing throughput, a scanning time of ~60 to 90 seconds is recommended for most soil applications. However, if lower LODs are essential, extending the scanning time can optimize pXRF performance. The Olympus® DELTA™ pXRF features several modes for analysis (Soil, Geochem, Mining, Alloy). These modes offer different packages of elements used in various applications. For most common soil science applications, Soil mode works quite well. More exotic studies of pollution sources or mine soil tailings may benefit from Mining or Alloy modes. In some instances, scanning with more than one mode can be useful, where certain elements are reported more accurately by one mode than another. These modes use various energies and filters to produce fluorescence signatures of various elements. The use of specialized filters may also enhance instrument performance for certain applications in which background scatter or interference can be isolated, allowing better performance [16].

SAMPLE APPLICATIONS AND CASE STUDIES, INCLUDING CALCULATIONS

To date, pXRF has been used to quantify elemental concentrations in several media [4]. While early pXRF studies focused on geologic, metallurgical, or archeological uses, newer soil science and agronomy applications have developed rapidly in recent years. Portable XRF is a good method for use in instances where the chemical properties of soils are of importance. Portable XRF will not provide LODs as low as traditional ICP–AES or ICP–MS analysis. Portable XRF reports total elemental concentration in soils, while techniques such as ICP–AES depend on the success of the digestion used to extract elements into solution. However, pXRF can provide *in situ* data of reasonable accuracy, with minimal to no sample

preparation in ~60 to 90 seconds. Also, pXRF may be useful in certain specialized applications where nondestructive analysis is required or matrices that do not lend themselves readily to traditional soil physicochemical analysis. Similar to spectral data collected by visible and near-infrared (VisNIR) spectroscopy, once collected, pXRF elemental data can be used to predict many physicochemical soil parameters. Universal predictive models can be used with some degree of accuracy, but for optimal results, it is advisable to collect pXRF elemental data, process the soil samples by traditional laboratory analysis, and then develop customized predictive models for a given area. In most cases, a customized model will show considerable accuracy across a given region as long as the general geological and soil properties remain similar. Importantly, the samples used in constructing the model should reflect the variability the investigator seeks to directly predict from the pXRF data. For example, if two substantively different soils are studied, two different models should be developed.

Most models are built on MLR, using elemental data as proxies for the parameter of interest. In developing the predictive model, the investigator should collect a robust dataset ($n \geq 100$ or more), reflective of all variability likely to be encountered in future analysis with the model. Randomly, 30% of the samples should be removed from the dataset for independent validation, with 70% of the samples used for model calibration. Calibration performances can be observed in terms of R^2 , RMSE, bias, residual prediction deviation, and ratio of performance to inter-quartile range.

Alternatively, concatenating pXRF elemental data with spectral data from other proximal sensors like visible VisNIR diffuse reflectance spectroscopy can be used in advanced algorithms like penalized spline regression (PSR), partial least squares regression, and random forest regression (RF) to predict several soil parameters with high accuracy [17]. The addition of remote sensing data has also been shown to increase model prediction accuracy [18]. Besides, an advanced combined modeling approach (PSR + RF) can be used in which PSR is used to fit the training set (containing VisNIR spectra only) using full cross-validation to choose the tuning parameter. Next, RF can be used to fit the residuals of the PSR model on the pXRF elemental data. The final predicted value represents the combination of PSR and RF predicted values [19].

REFERENCES:

- [1] C. B. Fliermans, T. D. Brock, *Soil Science* 1973, 115, 120.
- [2] USEPA, Method 3050B: Acid digestion of sediments, sludges, and soils, 1996, www.epa.gov.
- [3] USEPA, Method 3052: Microwave assisted acid digestion of siliceous and organically based matrices, 1996, www.epa.gov.
- [4] D. C. Weindorf, N. Bakr, Y. Zhu, *Adv. Agron.* 2014, 128, 1.
- [5] W. P. Gates, in *Handbook of clay science*, Elsevier, New York, 2006.
- [6] D. J. Kalnicky, R. Singhvi, *J. Hazard. Mat.* 2001, 83, 93.
- [7] D. C. Weindorf, N. Bakr, Y. Zhu, A. McWhirt, A., C. L. Ping, G. Michaelson, C. Nelson, K. Shook, S. Nuss, *Pedosphere* 2014, 24, 1.
- [8] A. Whirt, C. D. Weindorf, Y. Zhu, *Compost Sci. Util.* 2012, 20, 185.
- [9] S. Piorek, in *Current protocols in field analytical chemistry*, John Wiley & Sons, New York, 1998.
- [10] T. Radu, D. Diamond, *J. Hazard. Mater.* 2009, 171, 1168.
- [11] D. C. Weindorf, Y. Zhu, S. Chakraborty, N. Bakr, B. Huang, *Environ. Monit. Assess.* 2012, 184, 217.
- [12] A. Sharma, D. C. Weindorf, T. Man, A. Aldabaa, S. Chakraborty, *Geoderma* 2014, 232–234, 141.
- [13] A. Sharma, D. C. Weindorf, D. D. Wang, S. Chakraborty, *Geoderma* 2015, 239–240, 130.
- [14] S. Swanhart, D. C. Weindorf, S. Chakraborty, N. Bakr, Y. Zhu, C. Nelson, K. Shook, A. Acree, *Soil Science* 2014, 179, 417.
- [15] D. C. Weindorf, J. Herrero, C. Castañeda, N. Bakr, S. Swanhart, *Soil Sci. Soc. Am. J.* 2013, 77, 2071.
- [16] S. Bichlmeier, K. Janssens, J. Heckel, D. Gibson, P. Hoffmann, H. M. Ortner, *X-Ray Spectrom.* 2001, 30, 8.
- [17] D. D. Wang, S. Chakraborty, D. C. Weindorf, B. Li, A. Sharma, S. Paul, M. N. Ali, *Geoderma* 2015, 243–244, 157.
- [18] A. A. A. Aldabaa, D. C. Weindorf, S. Chakraborty, A. Sharma, *Geoderma* 2015, 239–240, 34.
- [19] S. Chakraborty, D. C. Weindorf, B. Li, A. A. A. Aldabaa, R. K. Ghosh, S. Paul, M. N. Ali, *Sci. Total Environ.* 2015, 514, 399.

02 Impact of Sample Preparation Methods for Characterizing the Geochemistry of Soils and Sediments by Portable X-Ray Fluorescence

K. Goff, R. J. Schaetzl, S. Chakraborty, *et al.*

ABSTRACT

We examined the impact of three different sample preparation methods on bulk soil geochemistry data obtained from a portable X-ray fluorescence (pXRF) spectrometer. We generated data from a soil core recovered from the surface, downward into unaltered loess, and into a buried soil at a site in eastern Iowa. Samples were scanned (i) directly from field-moist soil cores; (ii) after drying, grinding, and being loosely massed in plastic cups; and (iii) as pressed powder pellets. Data derived using these methods were compared with data obtained from a standard benchtop X-ray fluorescence (XRF) unit. Generally, the results indicated that data from pressed powder pellets provide the best correlation to benchtop XRF data, although the results were sometimes element- or compound-specific. CaO, Fe₂O₃, and K₂O generally provided the strongest correlations between pXRF and XRF data; SiO₂ data were more problematic. Field-moist pXRF scans generally underestimated element concentrations, but the correlations between pXRF and benchtop XRF measurements were greatly improved after applying pXRF-derived calibration standards. In summary, although element/compound data provided by pXRF showed significant relationships to benchtop XRF data, the results are improved with proper sample preparation and usually by calibrating the pXRF data against known standards.

INTRODUCTION

X-ray fluorescence (XRF) spectroscopy is an analytical technique used to determine the elemental composition of a sample using high-energy X-rays. When bombarded with X-rays, different elements can be identified by the characteristic fluorescent energy they emit (X-ray fluorescence). Thus, X-ray fluorescence offers a rapid and cost-efficient way to generate multielement analytical data.

Researchers are increasingly using portable X-ray fluorescence (pXRF) instruments in the field and laboratory ^[1]. Many studies have demonstrated that pXRF measurements correlate well with data obtained using conventional methods, such as benchtop XRF ^[2]. Portable XRF instruments can generate robust, accurate, and repeatable data and are applicable to various environmental applications ^[3].

As with any new method, researchers actively attempt to determine its overall accuracy and main error sources. Unfortunately, no universally agreed-upon protocol for pXRF sample preparation exists, specifically for analyses of soils or finely ground geological samples. Nonetheless, the Soil Survey Staff ^[4] has observed that the results from soil analyses are more reproducible if the sample has been air dried, homogenized, and finely ground (<75 μm). By comparison, the Soil Science Society of America method for pXRF analysis of soils advocates drying and grinding to pass a 2 mm sieve ^[5]. The present study addresses this issue by evaluating the effects of different sample preparation techniques on pXRF data.

For soil investigations, some studies have obtained data by placing the instrument directly onto a field-moist core ^[6]. Moisture in the sample attenuates the fluorescence, usually leading to underestimation of elemental data ^[7]. However, moisture levels of <20% generally cause a minimal error in elemental determinations ^[8]. For example, Stockmann et al. ^[6] calculated geochemical weathering indices using elemental pXRF data. Although the indices varied greatly between field-moist vs. dried samples, the depth trends showed similar patterns.

Although the accuracy of pXRF measurements from field-moist samples continues to be explored, most researchers conduct their analyses in a laboratory setting. Laboratory preparations typically involve combinations of drying, sieving, and grinding the samples before pXRF analysis ^[9]. Other

researchers physically compact each sample in a standard-sized container, forming a pressed powder pellet, before analysis.

Few studies have examined the efficacy of various sample pretreatments on the overall accuracy of the data. The objective of this study was to examine the effects of three different preparation methods on pXRF data from three soil samples: (i) field-moist soils, (ii) dried and ground powders, and (iii) pressed pellets. Data generated using these preparation methods were compared with traditional benchtop XRF data to determine the effects of sample pretreatment on final data accuracy.

METHODS

Samples from Clear Creek, a tributary of the Iowa River in eastern Iowa, were selected for the study. The Clear Creek Watershed is located within the Southern Iowa Drift Plain ^[10] and represents a hilly, dissected landscape underlain by Pre-Illinoian tills, with a mantle of loess. At the site, a 7.6 cm diameter core (5.0 m in length) was collected from a site on an upper shoulder slope. A detailed description of the study area and soil is present in the full article of this digest.

Three different pXRF preparation methods (field-moist condition, dried and ground to a powder, and pressed pellets) were compared to evaluate their efficacy for accurately determining soil/sediment geochemistry and weathering zones for the cores. A benchtop XRF unit was used as a comparative standard to establish the bulk chemical composition of the samples. Samples analyzed on the benchtop XRF had been initially removed from the scraped surfaces of the cores, dried at 50 °C (122 °F) for 12 hours, and ground to a fine powder. Subsamples of ~0.2–0.5 g were further ground to pass a 75 μm sieve, pressed into pellets, and made into homogeneous glass disks by fusion of the sample and a lithium tetraborate/lithium metaborate mixture ^[11]. XRF analyses were conducted for seven elements (Si, Al, Zr, K, Ca, Ti, Fe, and Mn) at SGS Canada Inc., in Mississauga, Ontario. Quality control was achieved using SiO₂ blanks, duplicates, and certified reference materials ^[11].

Portable XRF analyses were performed in Geochem Mode using an Olympus® DELTA™ Professional pXRF unit. The unit was operated on line at 110 VAC, without special filters, with a dwell time of 30 seconds, and under nor-

Table 1: Detection limits of the Olympus pXRF spectrometer for the seven elements reported in this study.

Analyzed element	Detection limit
Ti	10 ppm
Si	1.0%
Al	1.0%
Mn	10 ppm
K	50 ppm
Fe	10 ppm
Ca	50 ppm

mal atmospheric conditions. Instrument resolution was 150 eV per channel with a pulse density of 100,000 cps. Resulting waveforms were processed with the proprietary Olympus X-act Count Digital Pulse Processor and integrated software^[12]. Each time the pXRF was initialized, a 316 alloy coin was used for factory calibration. Detection limits for pXRF analyses vary by element (**Table 1**).

Initial scanning was completed by placing the pXRF device directly on the moist core at ≤ 10 cm intervals after any outer sediment material had been scraped away and the exterior area flattened with a knife. If a horizon break occurred, the sample increment was lessened so that no sample was taken from different horizon types. The remainder of the analyses were conducted on dried samples. In the laboratory, ~ 100 g samples were ground. Subsamples of ~ 20 g were then powdered, placed in 2.5 cm diameter plastic cups with at least 2 cm of material, covered with a 3.0 μm thin mylar film, and lightly tamped to achieve a level surface before pXRF analysis. Portable XRF analy-

ses were also conducted on pucks formed by compressing the sediment in 0.4×3 cm stainless steel cups using a stainless steel hydraulic press at 25 tons of pressure per square inch (pressed powder pellets). Four replicate scans were conducted on each sample for each method; all data reported are mean elemental data. Portable XRF data were converted to oxide values using standard conversion factors for SiO_2 , Al_2O_3 , K_2O , CaO , TiO_2 , Fe_2O_3 , and MnO . Four soil standard reference materials from the National Institute of Standards and Technology (NIST; <https://www.nist.gov/srm>; AGV-2, BIR-1, BCR-2, JA-1) were examined to develop linear calibration curves for selected elements/oxides using the Lucas-Tooth Calibration Method^[13]. The average value of each standard, based on five analyses, was then compared with the known values reported by Jochum *et al.*^[14]. An in-house standard of Peoria loess, which was geochemically similar to the core materials, was used as a fifth standard.

RESULTS AND DISCUSSION

Data derived from pXRF and benchtop XRF were often quite different; SiO_2 and Fe_2O_3 data were especially problematic (**Table 2**). Using three different sample preparation methods (moist core, dried and ground powder, and a pressed powder pellet), we sought to understand which method yields the most accurate pXRF results relative to data from the traditional benchtop XRF instrument. We assumed that benchtop XRF data most accurately characterize the overall bulk chemical composition of the soils. Benchtop XRF data may still suffer from overlapping fluorescence energies of different elements, limiting data interpretability. Furthermore, "light" elemental detection remains challenging given their weak fluorescent energies and atmospheric attenuation issues.

To that end, pXRF data from three different pretreatments were compared with benchtop XRF data. Example data from the Old Scotch core are shown in **Figure 1**. Generally, CaO , TiO_2 , and MnO data from the pXRF correlated best with benchtop XRF data, and for these compounds, the correlations were strongest when using the pressed powder method. Nonetheless, many of the data are element-specific, and thus the optimal sample preparation method is not the same for the seven elements/compounds. Portable XRF routinely overestimated the contents of Fe_2O_3 and Al_2O_3 and generally underesti-

Compound	pXRF	
	Benchtop XRF	(average of 55 runs)
	– wt% –	
Al_2O_3	8.71	8.13
SiO_2	70.30	52.24
K_2O	1.76	1.40
CaO	3.69	4.04
TiO_2	0.66	0.74
Fe_2O_3	2.96	3.80
MnO	0.07	0.07

Table 2: Elemental contents for an in-house standard of Peoria Loess, as determined by benchtop XRF and pXRF.

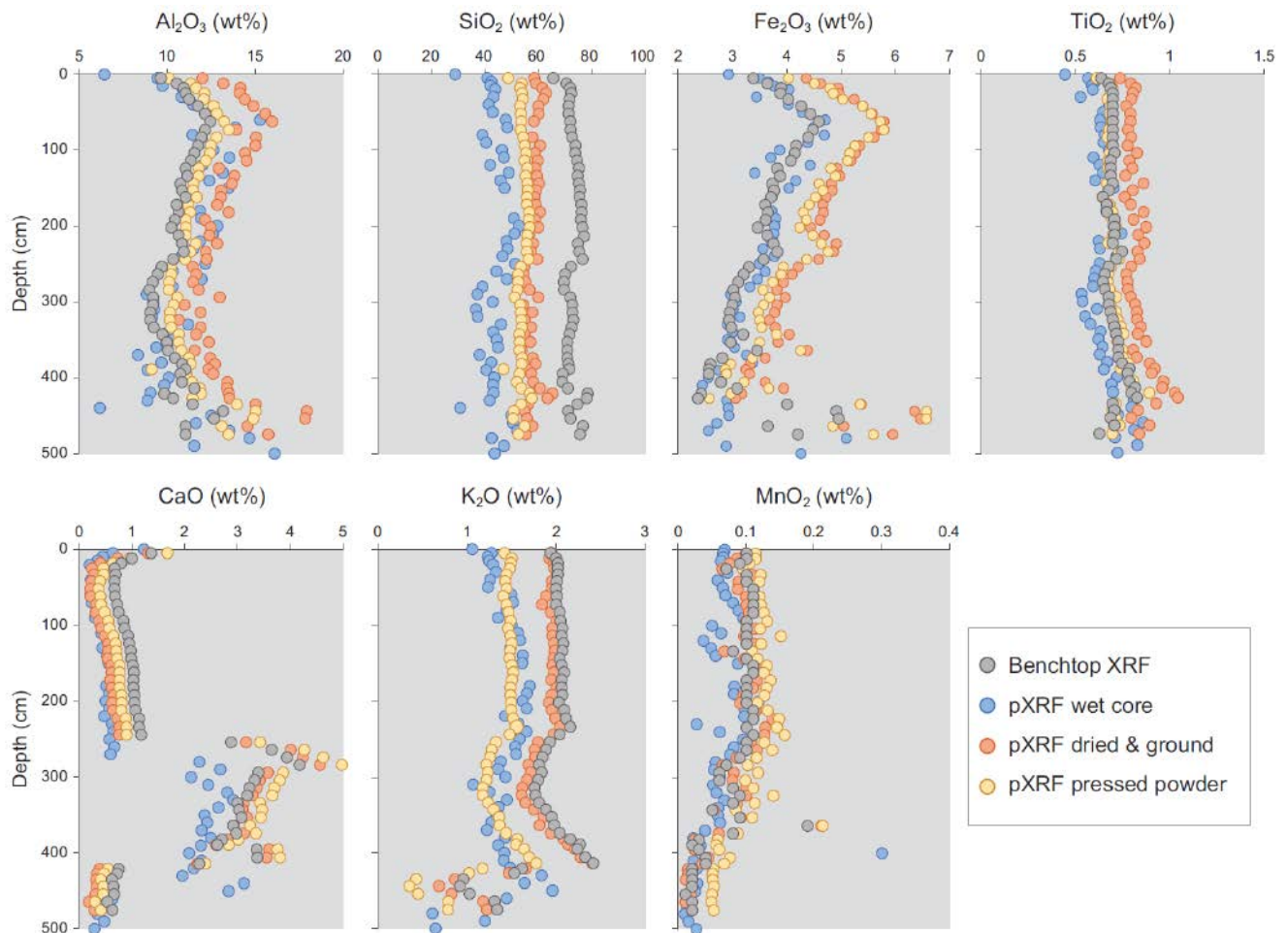


Figure 1: Depth plots of energy dispersive pXRF and benchtop XRF data for seven different oxides (Old Scotch core).

ated those of CaO and K₂O (**Figure 1**). Several researchers have reported a tendency of pXRF to overestimate Fe concentrations [15], a trend observed in the present study on all but the wet core samples (**Figure 1**). A possible explanation for the latter is that many closely spaced K- and L-lines occur in the low-energy region, causing spectral interferences [16]; however, as moisture attenuates fluorescence, that attenuation probably compensated for the overestimation of Fe in the present study. Generally, the accuracy of the data increased for most elements using the pressed powder pellet method. Thus, these data will be used as the pXRF component from this point forward.

Correlations of (pressed powder) pXRF vs. benchtop XRF data indicate that the highest *R*² values were obtained for CaO (0.997),

Fe₂O₃ (0.983), and K₂O (0.981); analyses for Al₂O₃ (0.746), TiO₂ (0.666), and SiO₂ (0.136) yielded lower correlations. Low correlation values for SiO₂ probably reflect variable attenuation of low-frequency X-rays during pXRF analysis, whereas the slightly lower correlation values for TiO₂ might reflect an uneven distribution of Fe-Ti oxides in the samples because of their overall lower concentrations.

Linear calibrations were developed for elements that appeared to vary consistently between benchtop XRF and pXRF analyses using four NIST standards and the in-house Peoria Loess standard (**Figure 2**). The linear regressions were then used to correct (calibrate) the pXRF data. Based on the standards shown in **Figure 2**, these calibrations are for major oxides: CaO, MnO, MgO, Fe₂O₃, P₂O₅, K₂O, and TiO₂. They produced well-correlated

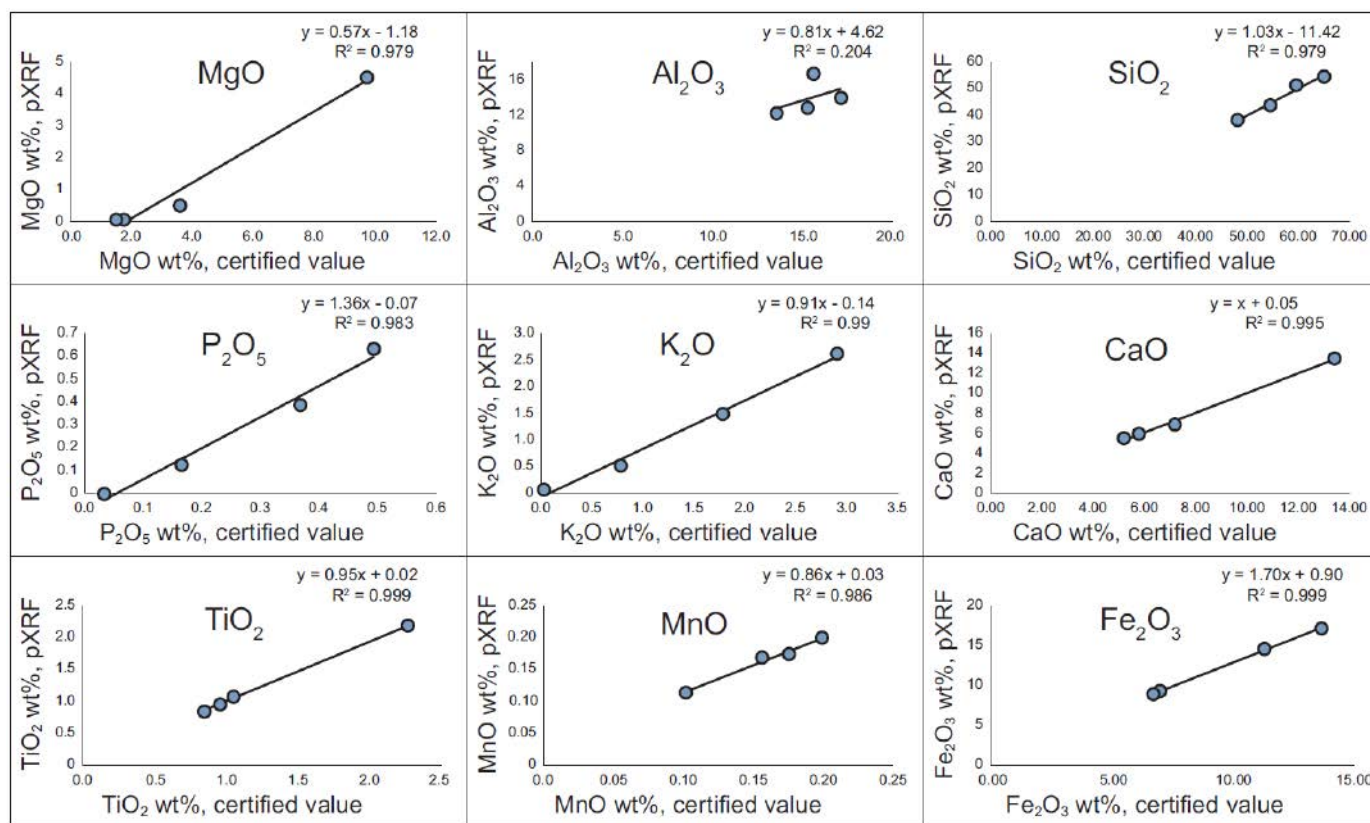


Figure 2: Calibrations developed for correcting energy dispersive pXRF data, using data from this study, four NIST standards, and an internal Peoria Loess standard.

Oxide	Equation	R^2	Equation	R^2
	Calibrated pXRF data		Raw pXRF data	
SiO_2	$y = 0.60x + 9.64$	0.60	$y = 0.35x + 31.92$	0.13
TiO_2	$y = 0.97x + 0.02$	0.72	$y = 1.25x - 0.04$	0.66
Al_2O_3	$y = 1.06x + 0.19$	0.72	$y = 1.37x - 1.40$	0.74
MnO	$y = 0.89x + 0.03$	0.90	$y = 1.07x - 0.004$	0.91
K_2O	$y = 0.94x - 0.47$	0.98	$y = 1.06x - 0.22$	0.98
Fe_2O_3	$y = 1.47x + 0.92$	0.98	$y = 1.30x - 0.06$	0.98
CaO	$y = 1.28x - 0.47$	0.99	$y = 0.88x - 0.41$	0.99

Table 3: Linear regression equations comparing calibrated and raw pXRF data to benchtop XRF data, using data from the Old Scotch core pressed pellet samples.

calibrations. Except for SiO_2 , the correlation coefficients are >0.7 , with most being >0.9 .

Table 3 illustrates the improvements in correlation between the uncalibrated vs. calibrated pXRF data of the samples. Although most of the data were improved using the calibration functions, data for some elements were only slightly improved or even slightly worsened. Despite producing substantial improvement in R^2 values for SiO_2 by pXRF correction, the concordance between benchtop XRF and calibrated pXRF SiO_2 data was still moderate at best ($R^2 = 0.60$). **Figure 3** shows the changes in the data for four elements obtained by applying the calibrations in **Figure 2** to the raw pXRF data.

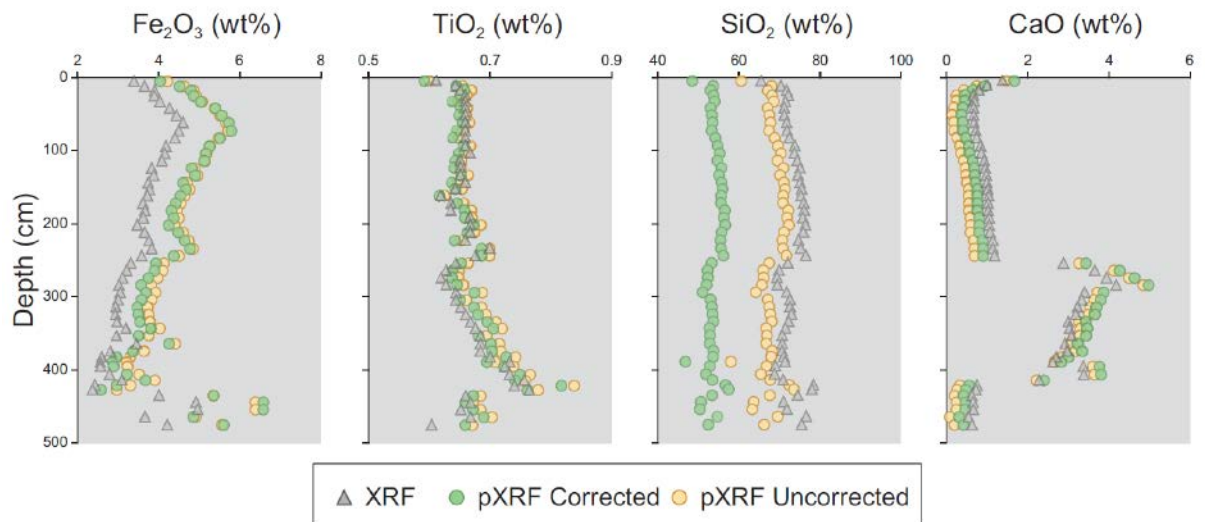


Figure 3: Depth plots showing agreement between calibrated and raw pXRF vs. benchtop XRF data for Fe_2O_3 , TiO_2 , SiO_2 , and CaO values for the Old Scotch core.

Results indicate that the overall accuracy of the Olympus® pXRF data is very good but somewhat element-dependent. For example, the comparatively poor performance of some elements may create problems for determining weathering ratios, many of which are dependent on Al or Si oxide contents and often use Ti as an indicator of the contents of the slowly weatherable mineral tourmaline [17]. Likely, the contents of light elements such as Mg, Al, and Si are more difficult to determine accurately because the emitted X-rays are more easily attenuated by the atmosphere. As a result, these elements have lower R2 values and poorer calibrations due to the low-energy condition and the inability of the current pXRF technology to properly correct this issue (Table 3).

The accuracy of raw pXRF data can be improved for most oxides by calibrations. Such linear calibrations should ideally have a slope of 1.0 and an intercept at the origin. The calibrations in this study differ significantly from these values, likely reflecting the inaccuracy of the internal calibration technique of the Olympus® instrument and issues related to X-ray attenuation, fluorescence, and interference. Thus, many pXRF data may have good correlations but are offset by XRF data derived from benchtop instruments (Figure 1). Improvements in these calibrations could be achieved using more standards and standards with higher variability in composition. Particularly concerning

is that applying calibrations to known standards did not improve the Si data (Figure 3).

The intensity of characteristic fluorescence decreases with increasing soil moisture due to strong X-ray absorption by soil water [5]. Therefore, dried, ground, and sieved soil samples should theoretically provide increased homogeneity by averaging out the effect of microscale inclusions and similar substances, such as Fe/Mn concretions. However, compression of dried/ground powders may also artificially inflate pXRF elemental readings by accentuating the number of atoms per unit area in contact with the X-ray beam. Indeed, the average bulk density of the pressed powder pellets was significantly higher (2.56 g cm^{-3}) than the average bulk density of the cores (1.69 g cm^{-3}).

CONCLUSION

In this study, soil/sediment samples from cores taken in loess soils in eastern Iowa were evaluated by pXRF spectrometry using three different pretreatments: (i) field-moist soils (no pretreatment), (ii) dried/ground powder, and (iii) pressed powder pellets. Results from the pXRF were compared with benchtop XRF data. Portable XRF data from pressed powder pellets performed best for certain elements/oxides and generally provided the strongest correlations between pXRF and XRF data. Data correlations for some other elements were less

robust. Scanning of field-moist samples consistently underestimated the concentrations of certain elements/oxides due to fluorescence attenuation. Therefore, soil samples should be dried, ground, sieved, and, in some cases, pressed into dense pellets before pXRF analysis.

Application of calibrations developed from standard materials to adjust pXRF data resulted in considerable improvements, leading to data that more closely align with bench-top XRF data. However, more work is needed to simultaneously consider the influence of moisture, sample bulk density, pXRF operational parameterization, and correction of reported pXRF data with local calibration samples. Those limitations notwithstanding, pXRF remains a powerful tool for rapid in situ analysis of soils and ground geologic sediments.

REFERENCES:

- [1] S. Chakraborty, B. Li, D. C. Weindorf, S. Deb, A. Acree, P. De, P. Panda, *Geoderma* 2019, 338, 5.
- [2] A. M. W. Hunt, R. J. Speakman, *J. Archaeol. Sci.* 2015, 53, 626.
- [3] D. C. Weindorf, N. Bakr, Y. Zhu, *Adv. Agron.* 2014, 128, 1.
- [4] *Soil Survey Staff, in Kellogg soil survey laboratory methods manual, Natl. Soil Surv. Ctr., Lincoln, 2014.*
- [5] D. C. Weindorf, S. Chakraborty, *Soil Sci Soc Am J.* 2020, 84, 1384.
- [6] U. Stockmann, S. R. Cattle, B. Minasny, A. B. McBratney, *Catena* 2016, 139, 220.
- [7] H. Sahraoui, M. Hachicha, *J. Fundam. Appl. Sci.* 2017, 9, 468.
- [8] USEPA, *Method 6200: Field portable X-ray fluorescence spectrometry for the determination of elemental concentrations in soil and sediment, 2007, www.epa.gov.*
- [9] B. M. Duda, D. C. Weindorf, S. Chakraborty, B. Li, T. Man, L. Paulette, S. Deb, *Geoderma* 2017, 298, 78.
- [10] J. C. Prior, *in Landforms of Iowa. University of Iowa Press, Iowa City, 1991.*
- [11] SGS Canada Inc., *Sample preparation and XRF procedure, Mississauga, 2016.*
- [12] Olympus Corporation, *XRF and XRD Analyzers DELTA Premium, Tokyo, 2017.*
- [13] M. J. Adams, J. R. Allen, *J. Anal. At. Spectrom.* 1998, 13, 119.
- [14] K. P. Jochum, U. Nohl, K. Herwig, E. Lammel, B. Stoll, A. W. Hofmann, *Geostand. Geoanal. Res.* 2005, 29, 333.
- [15] J. Koch, S. Chakraborty, N. Li, J. Moore-Kucera, P. Van Deventer, A. Daniell, C. Faul, T. Man, D. Pearson, B. Duda, C. A. Weindorf, D. C. Weindorf, *J. Geochem. Explor.* 2017, 181, 45.
- [16] D. Gallhofer, B. G. Lottermoser, *Minerals* 2018, 8, 320.
- [17] B. Buggle, B. Glaser, U. Hambach, N. Gerashenko, S. Markovic, *Quat. Int.* 2011, 240, 12.

03 Semiquantitative Evaluation of Secondary Carbonates via Portable X-Ray Fluorescence Spectrometry

S. Chakraborty, D. C. Weindorf, C. A. Weindorf, *et al.*

ABSTRACT

Secondary CaCO_3 is commonly found in soils of arid and semiarid regions in variable states of development. Historically, a qualitative scale featuring various stages of development has been applied when evaluating carbonate-laden soils. By contrast, this study used portable X-ray fluorescence (pXRF) spectrometry to determine the Ca concentration of 75 soil samples from four US states in relation to the developmental stage, as determined independently by five pedologists from the USDA–NRCS Soil Survey Staff. Although experienced, the evaluators unanimously agreed on the carbonate development stage of only 22.6% of the samples while evaluating the samples *ex situ*. Portable XRF-determined Ca content generally increased from Development Stage I through VI for intact aggregates and ground soil samples. The widest variation in Ca content was found in Stage III for both conditions. No substantive differences in Ca content were observed between Stages V and VI. A strong positive correlation was observed between the Ca content of intact aggregates vs. ground soil samples ($r = 0.89$). Both support vector machine classification, and interpretable rules were used to classify secondary carbonate development stages using total Ca concentrations for intact aggregates and ground soil. Using scans of both conditions offers stronger predictive ability than either condition independently. Portable XRF provides an important analytical tool for field soil scientists to evaluate soils containing Ca as part of CaCO_3 .

INTRODUCTION

Soils featuring secondary carbonates are common in semiarid and arid regions. CaCO_3 is a mineral of limited solubility, often originally derived from the mineral calcite or Ca-containing rocks. As mineral and rock forms of CaCO_3 degrade, they can serve as parent material for various soils. For example, Alfisols, Mollisols, and Inceptisols of the Southern High Plains of Texas are largely eolian in nature, and all contain substantive subsoil secondary CaCO_3 , originating from the northern Chihuahuan Desert (via prevailing winds from the south). The solubility of CaCO_3 is influenced by variable CO_2 pressure, pH, temperature, and salinity. Often in the presence of active acidity inher-

ited from atmospheric sources (e.g., H_2CO_3) or plant respiration, CaCO_3 dissolves to free Ca^{2+} and HCO_3^- ions that readily translocate within the soil as part of the soil solution^[1]. As water in the soil solution begins to evaporate, the solubility product is exceeded, and CaCO_3 begins to precipitate, leading to the development of lower portions of the solum as Bk, Bkk, Bkkm, Ck, or, more rarely, Ak horizons. Collectively, these horizons often constitute diagnostically recognized calcic horizons^[2].

The Soil Survey Staff commonly uses morphological attributes (e.g., identifiable carbonates) and qualitative descriptions of soil horizons for establishing the quantity of secondary carbonates observed either in a fine earth or coarse fragment matrix in the field (**Figure 1**)^[3]. Similarly, previous studies have investigated carbonates in soils, recognizing and describing up to six carbonate development stages^[4-6]. Although useful, these descriptions lack the objectivity of being quantitative measures. In contrast, CaCO_3 can be measured in the laboratory; however, the two most commonly applied methods—gasometry and titration—do not lend themselves easily to field quantification^[7].

Recently, portable X-ray fluorescence (pXRF) spectrometry has been shown to be adept at elemental quantification in situ. For example, using reagent-grade Ca under laboratory conditions, Zhu and Weindorf^[8] found an R^2 of 0.986 comparing pXRF-determined Ca levels with true Ca contents. The pXRF approach has also been successfully applied to enhanced pedon horizonation^[9], identification of lithologic discontinuities^[10], assessment of soil cation exchange capacity^[11], soil pH^[12], and salinity of both soil^[13] and water^[14]. The accuracy, speed, nondestructiveness, and inexpensiveness of pXRF offer formidable advantages over traditional laboratory-based analytical approaches^[15].

The pXRF approach cannot distinguish between the primary (rock/mineral) and secondary (BK/Bkk) source of Ca in CaCO_3 -containing soil horizons as it provides only elemental data on total Ca concentration. However, the enrichment of a soil horizon with CaCO_3 via pedogenesis may be assessed rapidly in situ. Such assessment is important for identifying diagnostic calcic horizons, which are defined by the CaCO_3 concentration relative to adjacent horizons. We hypothesized that total Ca contents in soil aggregates may provide insight into the pedogenic development stages of secondary

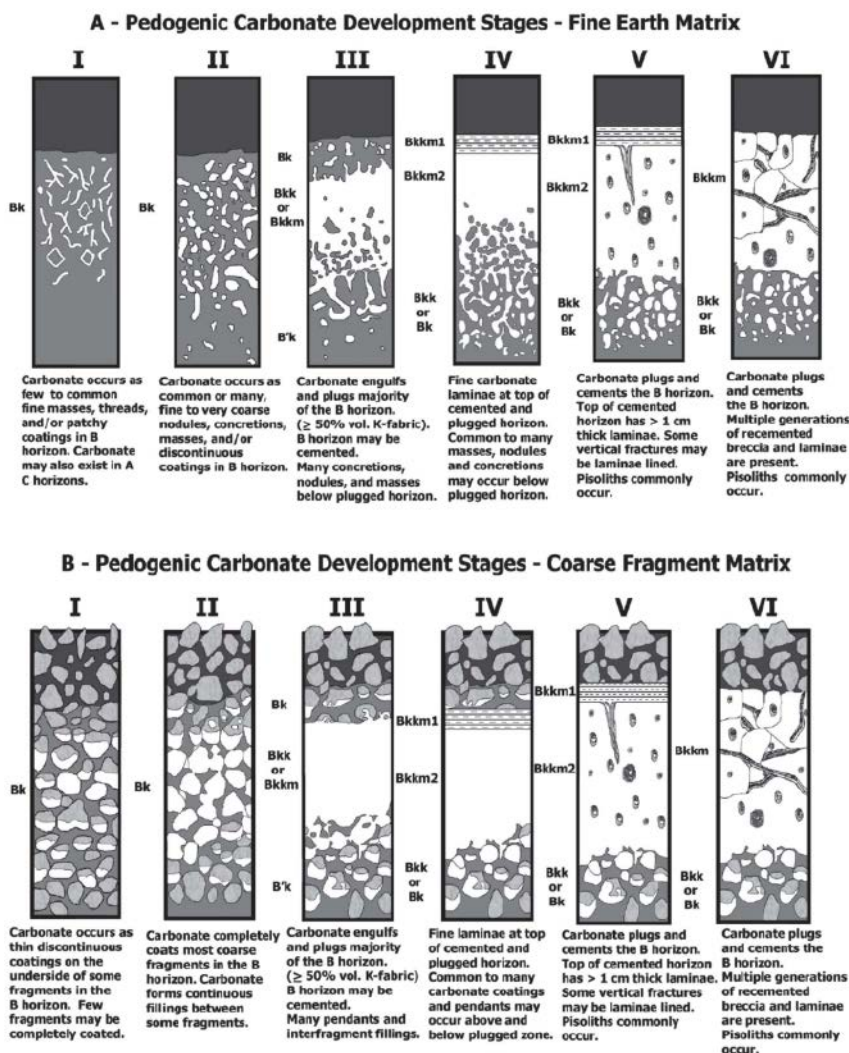


Figure 1: Pedogenic carbonate development stages for (A) fine earth matrix and (B) coarse fragment matrix^[3].

Parameter	<i>n</i>
<u>Sampling location</u>	
Colorado	
Colorado County	2
Kansas	
Decatur County	1
Norton County	2
Wallace County	12
New Mexico	
Chaves County	4
Lincoln County	16
Texas	
Garza County	6
Lubbock County	24
Scurry County	4
Yoakum County	4
Total	75
<u>Developmental stage</u>	
1.0–1.4	12
1.5–2.4	12
2.5–3.4	23
3.5–4.4	12
4.5–5.4	10
5.5–6.0	6
Total	75

Table 1: Qualitative assessment of secondary CaCO₃ development stage and sampling location of Bk, Bkk, Bkkm, and Ck horizons.

soil carbonates. Thus, we aimed to explore the extent to which pXRF-quantified Ca can explain secondary carbonate development stages.

METHODS

A total of 75 soil samples were collected across semiarid and arid regions of New Mexico, Texas, Colorado, and Kansas (**Table 1**). Sampling was done mostly in Bk, Bkk, Bkkm, and/or Ck horizons observed as road cuts. In some instances, soil pits were excavated to a depth of 1 m and then sampled. Soil sampling was done in accordance with [3], whereby subsoil aggregates were kept intact and placed in sealed plastic containers for transport to the laboratory.

LABORATORY ANALYSES

Upon receipt in the laboratory, samples were dried as intact aggregates for 5 days at 35 °C (95 °F) until air dry as soil moisture attenuates fluorescence [9]. With **Figure 1** provided as a reference, the secondary carbonate development stage of all samples was independently evaluated ex situ by five members of the USDA–NRCS Soil Survey Staff with a combined experience of 90 years. The rankings of each soil scientist were averaged to generate a mean score for each sample (**Table 1**). For comparative analysis, rounding of the mean score was performed to place a given sample into a class.

Ten selected soil samples were subjected to powder X-ray diffraction for mineralogical analysis. The 10 samples represented one sample from each county in which sampling occurred, and all six developmental stages were evaluated.

PORTABLE X-RAY FLUORESCENCE SCANNING

For pXRF, samples were scanned as intact aggregates using an Olympus® DELTA™ Premium (DP-6000) pXRF spectrometer. The spectrometer was positioned in a portable hooded test stand. Soil samples were placed on a Pro-lene thin film and positioned directly on the aperture of the pXRF, allowing for scanning of intact aggregates with irregular edges without exposure to stray X-rays. For samples showing considerable heterogeneity in secondary CaCO₃ distribution, the most carbonate-laden accumulation visible in the aggregate was scanned. Scanning was conducted in Geochem mode (two beams) at 40 seconds per beam, with elemental Ca as the target element of interest. After scanning all intact aggregates, samples were ground and rescanned as powders. Instrument performance was verified via the scanning of two NIST-certified reference soils.

Support vector machine (SVM) classification was implemented for statistical analysis to classify secondary carbonate development stages using total Ca concentrations in intact aggregates (Ca-intact) and ground soil (Ca-ground) samples. Radial kernel SVM was used, incorporating Ca-intact, Ca-ground, and Ca-intact + Ca-ground as explanatory variables. Tenfold cross-validation was used to select the optimal tuning parameters in SVM (cost and kernel width).

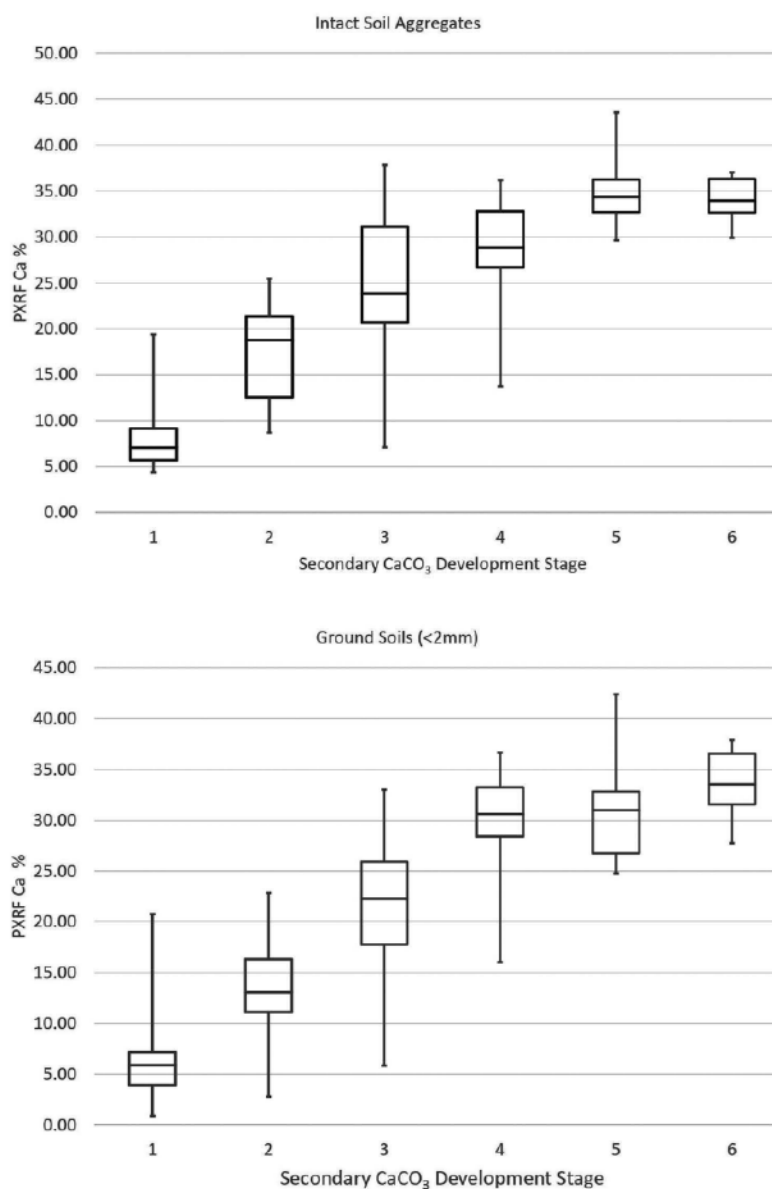


Figure 2: Median, quartiles, maximum, and minimum values of pXRF-Ca for Ca-intact (above) and Ca-ground (below) soils grouped by the visually determined developmental stages of carbonate-laden soils from Texas, New Mexico, Kansas, and Colorado.

Stage	Rule
I	{Ca.Intact – Ca.Ground > 0} AND {Ca.Intact + Ca.Ground < 20}
II	{Ca.Intact – Ca.Ground > 0} AND {20 < Ca.Intact + Ca.Ground < 40}
III	Variable
IV	{Ca.Intact – Ca.Ground < 0} AND {40 < Ca.Intact + Ca.Ground}
V	{Ca.Intact – Ca.Ground > 0} AND {55 < Ca.Intact + Ca.Ground}
VI	{60 < Ca.Intact + Ca.Ground}

Table 2: Rules for identifying six secondary carbonate development stages for carbonate-laden soils.

The full article of this digest includes a more detailed description of the SVM approach.

RESULTS AND DISCUSSION

Qualitative assessment of the secondary carbonate development stage showed considerable disagreement among the panel of evaluators. Unanimous agreement was found on only 16 samples (22.6%). Fair agreement was defined by one or more panelist(s) placing a given sample in adjacent carbonate development stages. Poor agreement was defined by panelists placing a given sample in three adjacent development stages. Fair and poor agreement among panelists was observed for 46 (61.3%) and 12 (16%) samples, respectively.

X-ray diffraction generally revealed a larger diversity in mineralogy and lower total Ca content at lower developmental stages. As the carbonate development stage increased, the mineralogy became increasingly dominated by CaCO_3 and SiO_2 . For example, a Stage III sample from Lincoln County, New Mexico, featured 42.6% CaCO_3 and 33.9% SiO_2 and included smaller quantities of phengite, anorthite, birnessite, and vermiculite. By contrast, a Stage VI sample from Lubbock County, Texas, featured 94.3% CaCO_3 and 5.7% SiO_2 ; no other minerals were identified.

Field-intact aggregate scans of soil Ca via pXRF showed clear differences between samples classified as carbonate development Stages I–V, with less difference between Stages V and VI (**Figure 2**). Importantly, pXRF reports only total soil Ca content, so it cannot distinguish between primary and secondary CaCO_3 or determine the degree of induration. Careful attention must be given to field-intact soil aggregates because secondary carbonate precipitation is often influenced by the wetting front, soil structure, and soil porosity^[4]. For example, it is quite common to find secondary carbonates deposited on the face of structural aggregates while the matrix remains carbonate-free^[16]. Thus, scanning the carbonate-laded prism face may cause an overestimation of the carbonate development stage relative to the overall soil volume. However, scanning soils both as intact aggregates and <2-mm powders provides an important differential measure that can be used for carbonate stage assessment (**Table 2**).

Pearson correlation testing exhibited a high positive correlation between Ca-intact and

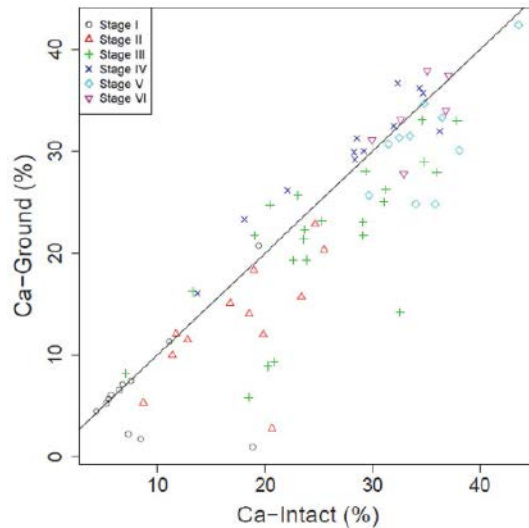
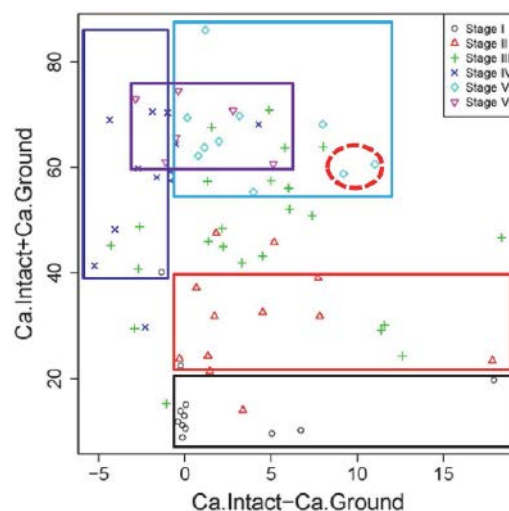


Figure 3: Scatterplot exhibiting correlation between Ca-intact and Ca-ground for carbonate-laden soils.

Ca-ground ($r = 0.89$, **Figure 3**). Moreover, **Figure 4** shows the basis for some interpretable rules (**Table 2**) that were devised for explaining different secondary carbonate development stages using Ca-intact and Ca-ground values. A box was used to identify each stage in the scatterplot. This was motivated by the fact that each box can be expressed by "IF AND THEN" language, with intervals on each variable. For example, Stage I's box can be expressed as IF (Ca-intact - Ca-ground is >0) AND (Ca-intact + Ca-ground is <20), THEN the sample is most likely to be Stage I (**Figure 4** and **Table 2**). Stage I was the easiest to identify, whereas Stage III was the most variable; these results are consistent with the variability

Figure 4: Scatterplot used for establishing the rules for explaining different secondary carbonate development stages for carbonate-laden soils.



observed in Ca content (**Figure 2**). Conversely, Stages IV–VI appeared very close (**Figures 2** and **4**). Notably, although Stages IV and V were very close to each other, Stage IV was above the $y = x$ line (**Figure 3**), indicating Ca-ground $>$ Ca-intact, whereas the opposite trend was observed in Stage V. These trends indicate the benefit of using both pXRF-sensed variables in classifying carbonate developmental stages. The results further indicate that pXRF scanning can be used to identify several carbonate developmental stages. Based on our results and the original concepts [3], revision to the carbonate development stages may be warranted. For example, Stages V and VI may be combined into a single developmental stage because their Ca content and morphological features were generally similar.

Using Ca-intact + Ca-ground, SVM achieved the lowest 10-fold cross-validation error (0.491). Conversely, while using Ca-intact and Ca-ground independently, SVM achieved 0.521 and 0.527 cross-validation errors, respectively. Hence, using two variables together provides better results than either variable alone. Notably, 83.3% ($n = 10$), 83.3% ($n = 10$), 91.03% ($n = 21$), 91.66% ($n = 11$), 60% ($n = 6$), and 33.33% ($n = 2$) of the samples were correctly classified for Stages I, II, III, IV, V, and VI, respectively. **Figure 5** shows the resultant nonlinear SVM classification plot. The region outside the data range is the extrapolation area, which is useless and artificial (e.g., yellow region in the top left corner). The plot indicates that Stage III (yellow region) had the largest area within the data range, indicating the largest variation for Ca-intact and Ca-ground. Further, the Stage I region (dark green) was mainly located at the lower-left corner, indicating that Stage I samples had the smallest Ca-intact and Ca-ground values. The Stage II region (green) is next to Stage I, confirming that samples from both groups were relatively close together. The Stage VI region (white) implies that Stage VI samples had the largest value in both variables. The narrow nature of the diagonal Stage V region can be attributed to the two samples from Stage V, which were close to the diagonal area (red circle in **Figure 4**). Further, Stages IV, V, and VI were relatively close to each other, exhibiting larger Ca-intact and Ca-ground values than Stages I and II (**Figures 2** and **4**). However, Stage IV and V were separated by the diagonal lines, implying that Stage IV samples had larger Ca-ground values than Ca-intact, whereas Stage V samples showed the opposite trend. Therefore, it can be concluded that Stages I and II were relatively easy to identify.

CONCLUSION

In summary, 75 carbonate-laden soils were subjected to pXRF scanning to provide semi-quantitative information on the carbonate development stage. The results indicate that Ca concentration increases steadily with the carbonate development stage. This was true for both intact aggregates and ground powder samples. Stage III carbonate development demonstrated the widest variability in Ca content. Intact aggregates showed almost no difference in Ca content between Stages V and VI. SVM analysis realistically classified carbonate development stages using total Ca concentrations in intact aggregates and ground soil samples. Portable XRF was generally shown to be a useful tool in establishing the developmental stage of secondary carbonates in soils.

REFERENCES:

- [1] C. C. Reeves, *J. Geol.* 1970, 78, 352.
- [2] Soil Survey Staff, in *Keys to soil taxonomy*, Natl. Soil Surv. Ctr., Lincoln, 2014.
- [3] P. J. Schoeneberger, D. A. Wysocki, E. C. Benham, E.C., in *Field book for describing and sampling soils*, Natl. Soil Surv. Ctr., Lincoln, NE, 2012.
- [4] H. W. Hawker, *Soil Sci.* 1927, 23, 475.
- [5] M. N. Machette, in *Calcic soils of the southwestern United States*, Geol. Soc. Am., Boulder, 1985.
- [6] A. M. Alonso-Zarza, P. G. Silva, J. L. Goy, C. Zazo, *Geomorphology* 1998, 24, 147.
- [7] R. H. Loeppert, D. L. Suarez, in *Methods of soil analysis. Part 3—Chemical methods*, SSSA and ASA, Madison, 1996.
- [8] Y. Zhu, D. C. Weindorf, *Soil Sci.* 2009, 174, 151.
- [9] D. C. Weindorf, Y. Zhu, B. Haggard, J. Lofton, S. Chakraborty, N. Bakr, W. T. Zhang, W. C. Weindorf, M. Legoria, *Soil Sci. Soc. Am. J.* 2012, 76, 522,
- [10] D. C. Weindorf, S. Chakraborty, A. A. Aldabaa, L. Paulette, G. Corti, S. Cocco, E. Micheli, D. Wang, B. Li, T. Man, A. Sharma, T. Person, *Soil Sci. Soc. Am. J.* 79, 1704.
- [11] A. Sharma, D. C. Weindorf, D.D. Wang, S. Chakraborty, *Geoderma* 2015, 239–240, 130.
- [12] A. Sharma, D. C. Weindorf, T. Man, A. A. Aldabaa, S. Chakraborty, *Geoderma* 2014, 232–234, 141.
- [13] S. Swanhart, D. C. Weindorf, S. Chakraborty, N. Bakr, Y. Zhu, C. Nelson, K. Shook, A. Acree, *Soil Sci.* 2014, 179, 417.
- [14] D. Pearson, S. Chakraborty, B. Duda, B. Li, D. C. Weindorf, S. Deb, E. Brevik, D. P. Ray, *J. Hydrol.* 2017, 544, 172.
- [15] D. C. Weindorf, N. Bakr, Y. Zhu, *Adv. Agron.* 2014, 128, 1.
- [16] R. J. Schaetzl, S. Anderson, in *Soils: Genesis and geomorphology*, Cambridge Univ. Press, New York, 2005.

05 Using EMI and P-XRF to Characterize the Magnetic Properties and the Concentration of Metals in Soils Formed over Different Lithologies

S. Doolittle, J. Chibirka, E. Muñiz, *et al.*

ABSTRACT

Two sites located in the Northern Piedmont of Pennsylvania suspected to have different levels of magnetic susceptibility (k) were examined using electromagnetic induction (EMI) and portable X-ray fluorescence (pXRF). One site is underlain by micaceous schist and serpentinite; the other site by micaceous schist only. The responses of an EM38-MK2-1 meter and the estimated k were greater and more variable at the site underlain by serpentinite and micaceous schist. Also, the average concentrations of Fe, Cr, Ni, and Ti were significantly higher at this site, and significant correlations were derived between the concentrations of several metals and the in-phase response and k of the upper 30 cm of the soil. These correlations were generally lower and less significant at the site underlain by micaceous schist alone. As k is associated with greater amounts of ferromagnetic constituents in soils, the greater concentration of Fe measured with pXRF at the site underlain by micaceous schist and serpentinite helps explain the greater averaged and more variable EMI responses measured with the EM38-MK2-1 meter at this site. The contrast in the EMI and pXRF data between these two sites was associated with differences in the mineralogy and lithologies of serpentinite- and nonserpentinite-derived soils.

INTRODUCTION

Little is known about the magnetic properties of soils and their spatial variability, but they are largely determined by the presence of iron oxides in different forms and concentrations ^[1]. The magnetic susceptibility (k) indicates the presence of iron-bearing minerals in soils and rocks. As k describes a material's ability to become magnetized, it is roughly proportional to the concentration of ferromagnetic minerals. However, the in-phase (IP) response of electromagnetic induction (EMI) sensors is also used to measure the magnetic properties of soils ^[2].

EMI surveys traditionally focus on the electrical properties of soils, neglecting the magnetic ones. In general, k of most soils is low and has negligible effects on electromagnetic field strengths; however, in magnetic soils, the presence of ferromagnetic minerals interferes with the efficiency of magnetic and electromagnetic sensors in detecting buried metallic objects ^[1].

The interpretation of k and IP data obtained from EMI sensors remains challenging due to various technical and environmental limitations, especially EMI sensor drift ^[3], arbitrary "zero level" ^[4], limited exploration depths ^[5], and changes in the sign (\pm) of the response at certain depths and in relation to the target position ^[6]. Regarding the latter, for EMI sensors operating in the vertical dipole orientation (VDO), the IP response experiences a sign change with depth ^[2]. For example, for the EM38 meter operating in the VDO, the response is positive for the upper 60 cm of the soil profile and weakly negative below 60 cm ^[2].

In the Piedmont of southeastern Pennsylvania and northeastern Maryland, areas of metamorphosed ultramafic rocks, which include serpentinite, occur along the state line ^[7]. Serpentinite is a Fe- and Mg-rich, subsiliceous rock formed principally through the metamorphic alteration of dunite, peridotite, or pyroxenite ^[8]. Soils formed over serpentinite have high Mg and low Ca levels, are low in essential nutrients, and have high concentrations of heavy metals ^[9]. During an EMI soil investigation conducted on a serpentine barren in southeast Pennsylvania, considerable variations in the IP and quadrature-phase (QP) responses were recorded. The cause of these unexpected results was attributed to the k of the soils formed over ultramafic rocks. As a result of these observations, a study was initiated to better understand the EMI response

on soils formed over different lithologies in the northern Piedmont of southeastern Pennsylvania and determine whether the concentrations of different metals in these soils could be linked to the response of an EMI meter and k .

METHODS

Two study sites, Nottingham Park (39.7375° N, 76.0326° W) and Cochranville (39.8735° N, 75.9315° W), were selected for this study. These sites are located about 12 miles apart in southwestern Chester County, Pennsylvania. The soils on these two sites formed over different lithologies. The Nottingham Park site consists of two portions (Glenelg and Chrome soils) and is located over ultramafic rocks and schist. The Cochranville site consists mainly of Glenelg soil is situated over schist. The full article of this digest includes a detailed description of both sites.

Pedestrian surveys were completed across each site with the EM38-MK2-1 meter (Geonics Limited) operated in the VDO and a continuous recording mode with measurements collected at a rate of 1 s⁻¹. The meter's long axis was orientated parallel to the traverse direction and held about 5 cm above the ground surface. Walking in a back and forth manner across each site along essentially parallel traverse lines, a total of 4465 and 4874 apparent electrical conductivity (EC_a) and IP measurements were recorded with the EM38-MK2 meter at the Nottingham Park and Cochranville sites, respectively. The Geonics DAS70 Data Acquisition System was used with the EM38-MK2-1 meter to record and store both EMI and GPS data. At the time of the EMI surveys, soils were moist throughout.

At each study site, a minimum number of soil sampling points were selected by submitting the IP EMI data to the Response Surface Sampling Design (RSSD) program of the ESAP (ECe Sampling, Assessment, and Prediction) software. RSSD was used to statistically select a small number of sample locations based on the observed magnitudes and spatial distribution of the IP EMI data; 12 and 7 optimal sampling points were identified at the Nottingham Park and Cochranville sites, respectively.

Two additional measurements were made at each of the optimal sampling points with the EM38-MK2-1 at different heights (0 and 150 cm). Using these data, k of the soil was estimated following the procedures of Geonics



Figure 1: Scanning a sample for elemental characterization with a pXRF spectrometer operated in benchtop mode.

Limited^[5]. Small grab samples were collected from the 0 to 30 cm and 30 to 60 cm depth intervals at each sampling point. The samples were dried and analyzed in sampling bags positioned at a constant distance from the portable X-ray fluorescence (pXRF) spectrometer mounted on a portable workstation (**Figure 1**). A DELTA™ Standard pXRF spectrometer (Olympus®) was used to determine the concentrations of 15 metals (K, Ca, Ti, Cr, Mn, Fe, Co, Cu, Zn, As, Rb, Sr, Zn, Ba, and Pb) in the samples from each site. The spectrometer was calibrated, and each sample was scanned for 60 seconds. For each sample, scans were repeated three times, and an average value was calculated.

	EC _a	IP	k
	mS m ⁻¹	ppt	10 ⁻⁶ x SI
Min.	2.58	-171.64	-2850
25%-tile	10.86	-30.00	869
75%-tile	17.07	17.03	9562
Max.	31.29	358.52	44802
Mean	14.26	1.81	9077
SD	4.77	55.42	13748

Table 1: Basic statistics for the EMI data collected at the Nottingham Park site.

RESULTS AND DISCUSSION

Electromagnetic Induction

A statistical summary of the EMI data collected at the Nottingham Park site is shown in **Table 1**. The EC_a averaged 14.3 mS m⁻¹, ranging from 2.6 to 31.3 mS m⁻¹. The comparatively low averaged EC_a was assumed to reflect the effects of soil weathering and the relatively shallow depths to bedrock. The IP data averaged 1.8 ppt, with an exceptionally large range of -172 to 359 ppt. The k averaged 9077 × 10⁻⁶, ranging from -2850 to 44802 × 10⁻⁶. The unusually large ranges in the IP response and k were attributed to the presence of iron-bearing minerals in soils and rocks. Similar variations have been observed in urban areas (e.g., anthropogenic soils) where the induced electric currents are significantly affected by the presence of metallic artifacts (e.g., pipes). No evidence was found of former structures, mining activities, or cultural deposits within the Nottingham Park site.

Figure 2 shows the spatial distributions of the EC_a and IP data collected at the Nottingham Park site. In each plot, segmented lineations with more extreme and anomalous values can be identified. These lineations suggest layers of contrasting lithology and mineralogy.

In the IP data plot (**Figure 2**), the higher amplitude (±) anomalies indicate "stronger" source objects. A "stronger" source object may be more conductive or magnetic, larger, and/or located closer to the surface. The amplitudes of the anomalies also depend on the source objects' orientation in the earth's magnetic field. This is especially true for elongate bodies such as veins of highly magnetic materials.

Table 2 lists the basic statistics for the EMI data collected at the Cochranville site. EC_a averaged 10.3 mS/m⁻¹, ranging from -0.1 to 15.5 mS m⁻¹. The IP data averaged -24.8 ppt, ranging from -48.0 to 10.1 ppt, and k averaged 1897 × 10⁻⁶, ranging from 798 to 5016 × 10⁻⁶. EC_a/IP measurements and k estimates were noticeably lower in magnitude and less variable at the Cochranville site than at the Nottingham Park site. The contrast in the EMI data between these two sites indicates differences in mineralogy and lithologies.

Figure 3 shows the spatial distributions of EC_a and IP data at the Cochranville site. Spatial patterns are nondescript except for a noticeable cluster of anomalous values in

Figure 2: Plots of the Nottingham Park site showing spatial variations in EC_a (QP component) and susceptibility (IP component). The soil line was imported from the Web Soil Survey. Numbers and point symbols on the IP plot label the locations of the twelve optimal sample points.

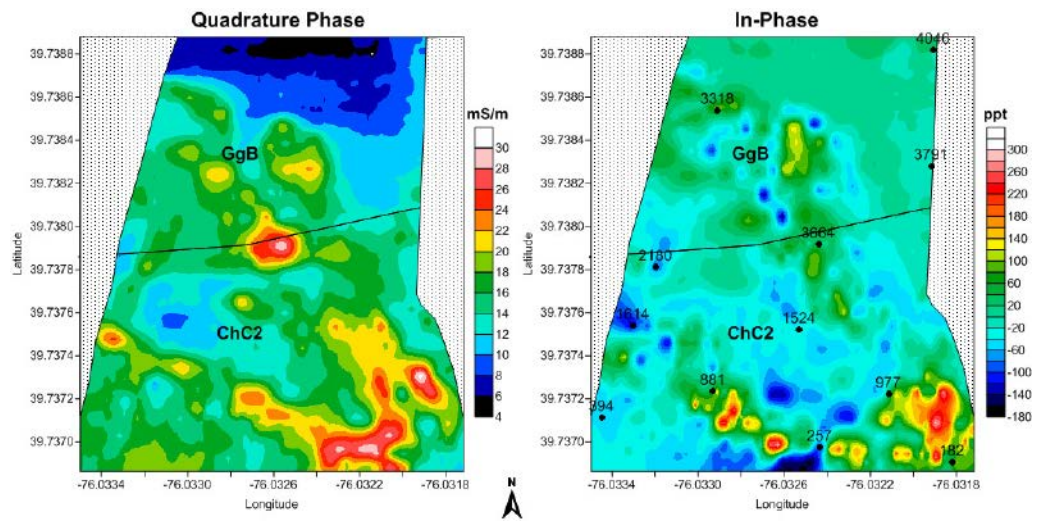
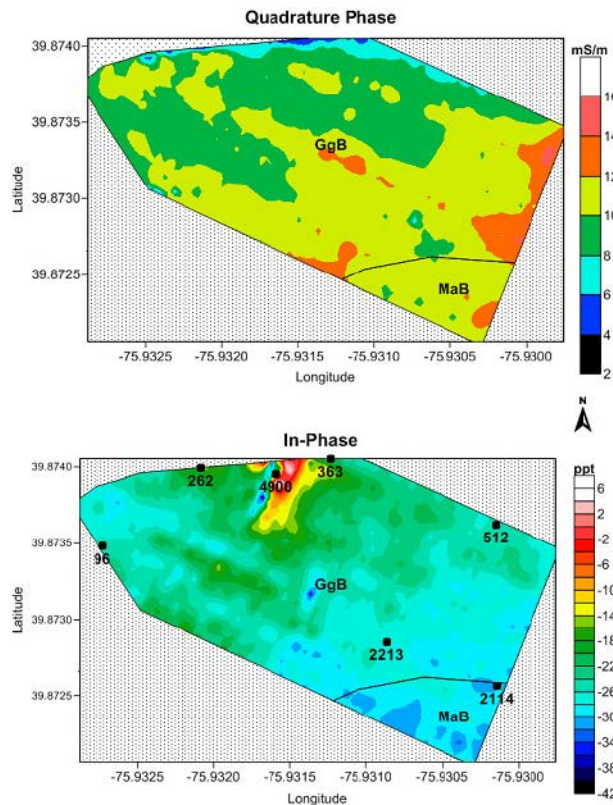


Figure 3: Plots of the Cochranville site showing spatial variations in EC_a (QP component) and susceptibility (IP component). The soil line was imported from the Web Soil Survey. Numbers and point symbols on the IP plot label the locations of the seven optimal sample points.



the extreme north-central portion of the site in the IP data plot. A small outcropping of the Peters Creek schist was evident in the vicinity of this anomalous pattern, and the area was associated with shallower depths to rock and contrasts in mineralogy.

X-Ray Fluorescence

At both sites, the concentrations of different metals varied over several orders of magnitude. Spatial and depth variability in these

concentrations was evident at each site. Noticeable differences in the concentrations of each metal were also evident between the sites. The full article of this digest contains tables with the concentration of every measured element in the samples collected at both sites and depth intervals. At both sites and depth intervals, Fe was the most abundant element. The average concentration of Fe increased with increasing soil depth. However, the average concentra-

	EC _a	IP	k
	mS m ⁻¹	ppt	10 ⁻⁶ x SI
Min.	-0.12	-47.97	798
25%-tile	9.41	-28.05	1112
75%-tile	11.29	-22.58	2052
Max.	15.51	10.08	5016
Mean	10.31	-24.76	1897
SD	1.67	4.95	1490

Table 2: Basic statistics for the EMI data collected at the Cochranville site.

tion of Fe for the 0- to 60-cm depth interval was about 152% higher at the Nottingham Park site than at the Cochranville site. At both sites, the concentration of Ca decreased with increasing soil depth. At the Nottingham Park site, the mapped Chrome soil is known for its low Ca/Mg ratios^[10]. However, the average concentration of Ca for the 0- to 60-cm depth interval was about 188% higher at the Nottingham Park site than at the Cochranville site.

The Chrome soil, which forms over serpentinite, typically has high Ni and Cr concentrations^[9,10]. The average concentration of Cr for the 0- to 60-cm depth interval was about 11 times higher at the Nottingham Park site than at the Cochranville site. Although less abundant, the average concentration of Ni was markedly higher at the Nottingham Park site than at the Cochranville site (960 and <20 mg kg⁻¹, respectively).

Correlation between EMI and P-XRF Data

Because of the small number of soil samples obtained from each site, nonparametric statistics were used to assess the relationship between EMI and pXRF data. **Table 3** summarizes the correlations between EMI and pXRF data for both depth intervals at the Nottingham Park site (only the eight most abundant metals are listed).

For the quadrature response (EC_a), correlations were mostly nonsignificant. However, a moderate and significant ($P = 0.05$) correlation was measured between EC_a and Mn. For the 30 to 60 cm depth interval, correlations between the different metals and EC_a were generally higher. Significant correlations were observed between EC_a and Cr, Mn, Fe, Co, and Ni. When operated in the VDO, the EM38-MK2-1 meter is relatively insensitive to materials at the surface, and its maximum sensitivity is at a depth of

	IP	k	K	Ca	Ti	Cr	Mn	Fe	Co	Ni
0–30 cm										
ECa	-0.139	-0.444	-0.140	-0.133	0.007	0.402	-0.699*	-0.255	-0.280	-0.039
IP		0.661*	-0.629*	0.496	-0.643*	0.608	0.853***	0.867***	0.881***	0.874
k			–	0.857**	-0.789	0.399	0.602	0.525	0.561	0.566
30–60 cm										
ECa	0.043	-0.354	-0.616	0.270	-0.470	0.639*	0.739**	0.684*	0.693*	0.711*
IP		0.625*	-0.546	0.325	-0.764*	0.427	0.491	0.418	0.382	0.654*
k			-0.148	0.325	-0.170	0.143	0.070	-0.084	-0.011	0.220

Table 3: Spearman's rank correlation coefficients for different EMI responses and element concentrations within the Nottingham Park site.

*, **, *** indicates significance at the $P = 0.055$, 0.01 , and 0.001 levels, respectively.

about 40 cm. This depth–sensitivity may partially explain the higher correlation between EC_a and the metals in the 30 to 60 cm depth interval. At the Nottingham Park site, for the 0 to 30 cm depth interval, strong and significant ($P = 0.001$) correlations can be observed between the IP response and the Mn, Fe, and Co contents. For the 30 to 60 cm depth interval, less significant and mostly lower correlations were obtained between the IP response and the concentration of various metals. The relative abundance of Fe in the Chrome and Glenelg soils and the relatively high correlation between IP response and this metal support the premise that the soils and underlying ultramafic rocks contain significant amounts of ferromagnetic and/or paramagnetic minerals that affect the response of EMI sensors.

For the samples obtained from the upper 30 cm at the Nottingham Park site, significant ($P = 0.01$) correlations exist between k and the concentration of Ca. Nonsignificant correlations were obtained between k and the concentrations of the other metals. For samples collected from the 30 to 60 cm depth interval, correlations between k and the concentrations of the measured metals were nonsignificant.

Table 4 lists the correlations between EMI and pXRF data at the Cochranville site. For the 0 to 30 cm depth interval, strong, negative, and significant ($P = 0.01$) correlations were obtained between EC_a and the Mn and Fe contents; however, this relationship cannot be explained at this time. For the 30 to 60 cm depth interval, correlations were mostly non-

significant between EC_a and the eight most abundant metals at the Cochranville site.

For both depth intervals, a significant correlation ($P = 0.05$) was obtained only between the IP response and Mn content. Compared with those at the Nottingham Park site, correlations were lower and nonsignificant between the IP response and Fe. Factors responsible for the lower and nonsignificant correlations may include lower Fe concentrations in the samples, effects of other physical parameters, and human-controlled variables related to differences in land management on the EMI response at the Cochranville site.

At the Cochranville site, significant correlations were obtained between k and the concentrations of Mn and K/Mn in the 0 to 30 cm and 30 to 60 cm depth intervals, respectively.

CONCLUSION

This study determined and associated the concentrations of different metals in soils formed over different lithologies in the Northern Piedmont of southeastern Pennsylvania with the responses of an EMI meter. The IP and QP responses of an EM38- MK2-1 meter and the estimated k were greater and more variable at the site underlain by micaceous schist and serpentinite than those at the site underlain by micaceous schist alone. The contrast in the EMI response and k between the two sites was associated with mineralogy and lithology differences. Spatial and depth variabilities in metal concentrations were evident at each

	IP	k	K	Ca	Ti	Mn	Fe	Co	Zr	Ba
0–30 cm										
ECa	–0.509	–0.705	–0.547	–0.278	–0.402	–0.848*	–0.759*	–0.277	0.723	–0.045
IP		0.911	0.446	0.643	0.357	0.821*	0.482	0.232	–0.393	0.250
k			0.536	0.571	0.464	0.857*	0.571	0.214	–0.714	0.107
30–60 cm										
ECa	–0.714	–0.589	–0.750	0.321	–0.107	–0.750	–0.536	–0.027	0.464	–0.598
IP		0.911	0.750	–0.143	0.000	0.786*	0.607	–0.027	–0.357	0.402
k			0.875**	0.071	0.375	0.821*	0.679	0.179	–0.571	0.232

Table 4: Spearman's rank correlation coefficients for different EMI responses and element concentrations within the Cochranville site.

*, ** indicates significance at the $P = 0.055$, and 0.01 levels, respectively.

site. Noticeable differences in the concentrations of each metal were also evident between the sites. Fe was the most abundant metal at both sites. However, the average concentration of Fe for the 0 to 60 cm depth interval was about 152% higher at the site underlain by micaceous schist and serpentinite than that at the site underlain by micaceous schists alone. At the first-mentioned site, for the 0 to 30 cm depth interval, strong and significant correlations were observed between the concentration of several metals and the IP response and k . These correlations were lower and mostly nonsignificant at the site underlain by micaceous schists only. For both sites, the correlations between the various metals and EC_a were mostly nonsignificant. The contrast in the EMI and pXRF data between these two sites was largely associated with differences in k , mineralogy, and lithologies.

REFERENCES:

- [1] R. L. Van Dam, J. M. H. Hendrickx, B. Harrison, B. Borchers, D. J. Norman, S. Ndur, C. Jasper, P. Niemeje, R. Nartney, D. Vega, L. Calvo, J. E. Simms, *Proc. SPIE*. 2004, 5415, 665.
- [2] R. Dalan, in *Remote Sensing – Applications*, Alabama Press, Tuscaloosa, 2006.
- [3] A. Tabbagh, in *Seeing the Unseen—Geophysics and Landscape Archaeology*, Taylor & Francis Group, London, 2009.
- [4] R. E. North, J. E. Simms, *SAGEEP 2007*, 20, 264.
- [5] Geonics Limited, *EM38-MK2-1 ground conductivity meter operating manual*, Geonics Ltd., Mississauga, 2009.
- [6] A. Tabbagh, *Archaeometry* 1986, 28, 185.
- [7] M. L. Crawford, W. A. Crawford, A. L. Hoersch, M. E. Wagner, in *The Geology of Pennsylvania*, Pennsylvania Geological Survey and Pittsburgh Geological Society, Harrisburg, 1999.
- [8] J. D. Istok, M.E. Hayward, *Soil Sci. Soc. Am. J.* 1982, 46, 1106.
- [9] J. L. Burgess, S. Lev, C. M. Swan, K. Szlavecz, *Northeastern Naturalist* 2009, 16, 366.
- [10] M. C. Rabenhorst, J.E. Foss, *Soil Sci. Soc. Am. J.* 1981, 45, 1160.

XRF and XRD Instruments for Geoscience



Both X-ray fluorescence (XRF) and X-ray diffraction (XRD) are frequently used analysis techniques for the analysis of rock, sediment, and other earth material samples. Geoscientists in the field use portable equipment to get real-time material chemistry (XRF) and mineralogy (XRD) of geo-logical samples as well as microscopes for traditional optical mineralogy and petrology. You can learn more about the functional principles of these instruments in the introduction on page 3.

XRF is a powerful, nondestructive technique for measuring elemental composition from magnesium (Mg) to uranium (U), from parts per million to 100%. Compact and portable XRF machines offer accurate, rapid elemental analysis on the go, making them an essential piece of equipment for anyone looking for laboratory quality results. Prescreening using XRF enables priority sample selection for laboratory analysis, maximizing analytical budgets.

Whereas XRF instruments are used for the quantification of a specific element, XRD analyzers can identify and quantify crystalline compounds or phases in a sample. Portable XRD instruments allow the identification of all mineral phases in the field in realtime. Both complimentary methods together allow the coverage of large areas very quickly and enable users to make decisions in the field.





Five XRF Accessories for Mining and Geochemical Analysis Field Kit Handheld XRF analyzers can provide immediate, onsite elemental measurements for a range of mining and geochemical analysis applications, including mineral exploration, ore grade control, and environmental monitoring.



1. VANTA WORK STATION

The Vanta Work Station is a fully interlocked system that enables you to set up your handheld XRF analyzer on a benchtop or as a portable field laboratory. Simply power on the system, click the analyzer into place, close the lid, and start the test through a wireless connection or USB. While the test runs, you can perform other tasks and stay productive.



2. VANTA SOIL FOOT

Another helpful tool for hands-free analysis is the Vanta Soil Foot, which provides a stable three-point support for your XRF analyzer. This compact, cost-effective accessory is useful for the longer test times required in some mining and geochemical analysis applications.



3. VANTA FIELD STAND

If you need to test small items such as samples in cups or bags, then look no further than the Vanta Field Stand. The lightweight, portable test stand and shielded sample chamber are easy to set up, use, and pack away in just a few steps.



4. VANTA HOLSTER

Keep your XRF analyzer securely by your side and ready when you need it with the Vanta Holster.



5. VANTA TRANSPORT CASE

All Vanta handheld XRF analyzers come with a rugged, hard-shell transport case that can endure tough mining and field conditions. But if you ever need a replacement, just head to our web-store to order a new case.

You can find all mining and geology solutions of Olympus at <https://www.olympus-ims.com/en/solutions/mining-geology>